ATTENUATION RELATIONSHIP FOR NORTH-EAST INDIAN REGION

A DISSERTATION

Submitted in the partial fulfillment of the

requirements for the award of the degree of

MASTER OF TECHNOLOGY

in

EARTHQUAKE ENGINEERING

(With specialization in Seismic Vulnerability and Risk Assessment)

By

SUSHANT CHAUHAN

(17553008)

DEPARTMENT OF EARTHQUAKE ENGINEERING

INDIAN INSTITUTE OF TECHNOLOGY ROORKEE,

ROORKEE– 247667 (INDIA)

June 2019

CANDIDATE'S DECLARATION

I, Sushant Chauhan hereby declare that the work which is being presented in the dissertation entitled **"ATTENUATION RELATIONSHIP FOR NORTH-EAST INDIAN REGION"** in partial fulfillment of the requirement for the award of degree of Masters of Technology in Earthquake Engineering with specialization in Seismic Vulnerability and Risk Assessment, and submitted to the Department of Earthquake Engineering, Indian Institute of Technology, Roorkee, is a record of my own work carried out during the period from July 2018 to June 2019 under the supervision of **Dr. S.C. Gupta,** Associate Professor in the Department of Earthquake Engineering, Indian Institute of Technology Roorkee, Roorkee, India.

The matter embodied in this dissertation has not been submitted by me for the award of any other degree.

Place: Roorkee **(SUSHANT CHAUHAN)**

Date: (17553008)

CERTIFICATE

This is to certify that the above statement made by the candidate is correct to the best of our knowledge and belief.

Place: Roorkee **(DR. S.C. GUPTA)**

Date: Associate Professor

Department of Earthquake Engineering

Indian Institute of Technology Roorkee

ACKNOWLEDGEMENT

I would like to take this opportunity to express my sincere and profound gratitude to my guide **Dr. S.C. Gupta**, Associate Professor in Department of Earthquake Engineering, Indian Institute of Technology Roorkee for his precious guidance, encouragement and invaluable suggestions at every stage of this dissertation. It would not have been possible to complete this work in time without his co-operation.

I express my gratitude to all the faculty members, Earthquake Engineering Department for their valuable suggestions at various stages of work.

I am grateful to **Ms. Neha Kumari** - Research Scholar for her constant advices and timely support. I would also like to thank my batch mates and friends.

I express my heartfelt gratitude to my parents for their constant encouragement, blessings, inspiration, and support throughout the study.

I am highly indebted to the whole department of Earthquake Engineering, IIT Roorkee for all the facilities extended throughout this work.

ABSTRACT

Ground motion attenuation relationship is the most significant and useful topic in engineering seismology. It provides the background for seismic resistant design, seismic zonation map and seismic hazard analysis. Based on strong motion data of Himalayan region, ground motion attenuation relationships were scarcely found in public literatures. And most of the previous attenuation relationships took intensity as an objective, also without consideration of site conditions. In this thesis, strong motion data of North-East Indian region are collected to develop the seismic parameter, e.g. peak ground horizontal acceleration based attenuation relationships and the predictive equations are presented herein.

An important component of seismic hazard analysis is to provide a proper model used for predicting the expected ground motion distribution for a possible earthquake scenario, which should consider the characters of earthquake sources, the paths of wave propagation and local site conditions. In this thesis, 254 earthquake recordings were selected with 2 horizontal orthogonal-component seismograms i.e. N-S and E-W, both from National Strong Motion Instrumentation Network database. The widely used ground motion attenuation model is adopted to construct the empirical attenuation equations by two-step regression method proposed by Joyner and Boore [1981]. The predicted peak ground parameters are expressed as a function of magnitude, distance (hypocentral distance) and site category. The model uses a magnitude-independent shape according to geometrical spreading and anelastic attenuation for the attenuation relationships. The final results then are compared with previous attenuation equations proposed for this area.

TABLE OF CONTENTS

LIST OF FIGURES

LIST OF TABLES

Chapter 1 INTRODUCTION

1.1 General

Earthquakes are unpredictable and disastrous. Though we can determine the range of area, time and magnitude of earthquake but we cannot predict the exact place, time and magnitude. They are causing catastrophic damage to structures and property and tremendous loss of lives of human beings. This is the reason why there is a need to study earthquake and seismology. We can decisively say about the future earthquakes only if we study as large number of earthquakes as possible. For this we need numerous high quality recording stations spreading appropriately over the study area which can give us high quality seismic data. On applying the inverse analysis on the sufficiently available data we can predict about the nature of the future earthquake events and how they may propagate in the surrounding areas. The idea of reducing earthquake hazard by building earthquake resistant structures is strongly backed up by identifying earthquake prone areas and how much shaking they may produce.

These installed stations record the seismic data in the form of ground motion as a graphical representation varying with time which are called as seismograms. Out of the three orthogonal components of seismograms two horizontal components are used in this thesis for the estimation of ground motion attenuation relationships.

Earthquakes caused structural damage in earthquakes. During seismic events, seismic waves are generated from points in all directions called sources and then propagated within the earth's crust. When they reach the surface of the earth, they cause vibration. This vibration can last for a few seconds to a minute.

Hazards caused by earthquakes are classified in two categories i.e. primary hazards and secondary hazards. Primary hazards are those caused directly by earthquakes and secondary are those which are caused by primary hazards. Hence to reduce the losses caused by these hazards, tremendous work is being done in this field related to hazard estimation and mitigation. Estimation of attenuation relationship is one of the primary step in these studies.

Table 1.1 Hazard categorization

PRIMARY EARTHQUAKE HAZARDS	SECONDARY EARTHQUAKE HAZARDS
• Ground Shaking	• Tsunamis
• Landslides	• Seiche
• Liquefaction	• Flooding
• Surface Rupture	• Fire

1.2 Importance of the study

Earth Science and Structural Engineering are two very important aspects of Earthquake Engineering. Engineering Seismology acts as a link between them. Engineering Seismology gives contribution by providing with loading conditions which satisfy conditions pertaining to the level and frequency of the structures in their lifetime.

These loading conditions can be estimated through certain equations which are based on strong motion data available from previously recorded Earthquake events. These equations may be and are being used for a very large area but if possible, site specific equations can be used to get more accurate results. One of the biggest problem in this is the unavailability of sufficient number of recordings with appropriate and required characteristics. Thus we need a predictive model popularly known as attenuation relationship which is a mathematical function which sets up a relation between a strong motion parameter and parameters which characterize earthquake, medium of propagation, geology of local site and structural parameters. Dependent parameters are like peak ground horizontal acceleration, peak ground vertical acceleration, spectral acceleration, etc. and the independent parameters are like magnitude, distance from the source, etc. The coefficients of the parameters in the relationship are determined with the help of regression analysis.

These relationships are not a mere tool of estimating the ground motion variation with respect to the distance but has a major role in the earthquake hazard analysis of any area. Hence these equations can play an important role in accurate estimation of ground motion and subsequently designing our structures accordingly.

Chapter 2 LITERATURE REVIEW

A brief description of different studies done in this field is given below:

Esteva (1970) gave ground motion model as:

$$a = 1230\, e^{0.8M}\, (R + 25)^{-2} \tag{2.1}$$

where a is in cm/s^2 and standard deviation is 1.02 (in natural log).

Records were taken from sites of stiff clay or hard conglomerate and earthquakes events of moderate durations were considered.

Ambraseys (1975) gave ground motion model as:

$$\log Y = 0.46 + 0.63\, M_L - 1.10 \log R \tag{2.2}$$

where Y is expressed in cms^{-2} and standard deviation is 0.32.

Earthquakes with maximum focal depth of 15 km were used.

McGuire (1978) gave ground motion model as:

$$\ln x = 3.40 + 0.89M - 1.17 \ln R - 0.20Y_S \tag{2.3}$$

where x is in cm/s^2 and standard deviation is 0.62.

Used two site class:

Ys = 0 for sedimentary/basement rock or soil of less than 10m depth, 11 records.

Ys = 1 for alluvium/soft material of greater than 10m depth, 59 records.

Records were taken from basements of buildings otherwise from free field. Not greater than 7 records from a single earthquake event & not greater than 9 records of one specific site were considered to reduce underestimation of the obtained variance.

Cornell et al. (1979) gave the relationship as:

$$\ln A_P = 6.74 + 0.859M_L - 1.80 \ln(R + 25) \tag{2.4}$$

here A_P is in cms^{-2} and standard deviation is 0.57.

Not > 7 records from an earthquake event were taken to reduce the biasing in the results obtained. Records were taken from building's basements/free field.

Sabetta and Pugliese (1987) gave relationship as:

$$\log y = -1.562 + 0.306\, M - \log(R^2 + 5.8^2)^{1/2} + 0.169S \tag{2.5}$$

where y is in terms of acceleration due to gravity g & standard deviation is 0.173.

Used two site class:

S = 0 Stiff soil of depth greater than 20 m, 74 records.

S = 1 soft soil of depth between 5 m and 20 m, 21 records.

Petrovski and Marcellini (1988) gave relationship as:

$$\ln (a) = 6.48 + 0.544\, M - 1.33 \ln(R + 20) \quad (2.6)$$

where a is in cms^{-2} & standard deviation is 0.67.

Greece, Italy and Yugoslavia were the study areas. Focal depth of not greater than 40 km was considered.

Sharma (1998) gave relationship as:

$$\log A = -1.072 + 0.3903\, M - 1.21 \log(X + e^{0.5873\, M}) \quad (2.7)$$

where A is in g and X is in km and standard deviation is 0.14.

66 PGAs from 5 earthquake events were used as a database.

Two site class were considered but were not modelled:

Rock site, 41 records.

Soil site, 25 records.

7.0 < Focal depth < 50.0 km was considered. Majority of records were from distances greater than 50 km. Source mechanism as parameter was not considered. Type of the tectonics was neglected. Weighted regression was used. Suggested that lack of data can make the equation unreliable. And as a conclusion it was stated that this equation gives lesser values at shorter distances.

Chapter 3 SEISMOTECTONICS OF THE STUDY AREA

The Himalayas are formed by the subduction of Indian tectonic plates beneath the Eurasian plate, extending from southwest to northwest over 2,400 km long, width of 400 km in the west and 150 km in the east. Some of the world's highest peaks are located in Himalayas including the highest peak in the world i.e. Mount Everest (8848 m).

The study area of North-East Indian region has Archean landmass and has tertiary Himalayan mountains in the north and Indo-Burman folds in east and south-east. This region has gone through multiple deformational phases. It has rugged terrain except the Brahmaputra valley plains which are flooded annually.

The Himalayan Region is seismically very active. The north-eastern Himalayan region is one of the six most seismically active regions of the world after Mexico, Taiwan, California, Japan and Turkey. 18 large earthquakes ($M \geq 7$) have happened in the region in last 100 years which includes Shillong earthquake (1897, M_w=8.0) and Assam earthquake (1950, M_w=8.7). This region lies in seismic zone IV and zone V as per IS Code (IS 1893 (Part 1): 2002). Seismotectonic study of this area is essential as it is useful in analysis of seismic patterns, earthquake source mechanism and hazard estimation of a region. The study area extends from latitude 23°N to 30°N and longitude 89°E and 98°E. This covers seven sisters of India (Arunachal Pradesh, Assam, Meghalaya, Manipur, Mizoram, Nagaland, and Tripura) and adjoining areas of Bhutan, China, Myanmar and Bangladesh.

Structure of north-east Indian region can be divided into the following -

I. the overthrust eastern Himalayas,
II. the overthrust Naga Hills including the Patkai-Kohima synclinorium,
III. the Assam valley extending from Shillong plateau to Upper Assam,
IV. Shillong plateau and Mikir Hills,
V. Surma valley,
VI. Arakam-Yoma folded belts.

Table 3.1 Division of Seismogenic Sources in North Eastern Indian Region

Sl. No.	Seismogenic Zone	Major division	Subdivision
1	SZ-I	East West Trending Features	Eastern Himalaya
2	SZ-II	Eastern Syntaxis	Eastern Syntaxis
3	SZ-III	Shillong Massif	Shillong Plateau
4	SZ-IV	Shillong Massif	Dauki Fault
5	SZ-V	Shillong Massif	Sylhet Fault
6	SZ-VI	North South Trending features	Naga Disang Thrust
7	SZ-VII	North South Trending features	Eastern Boundary Thrust (I)
8	SZ-VIII	North South Trending features	Eastern Boundary Thrust (II)
9	SZ-IX	North South Trending features	Eastern Boundary Thrust (III)
10	SZ-X	North South Trending features	Mat Fault

The northern side of north-east Indian region i.e. plate boundary between India and China and eastern side of this region i.e. plate boundary between India and Myanmar are, in reality, plate boundaries between Indian and Eurasian plate. This is a part of Alpine belt which extends from Spain to Indonesia.

The Himalayas are constituted of thrust planes namely the Main Central Thrust (MCT), Main Boundary Thrust (MBT), Main Frontal Thrust (MFT). Plate motion over Po Chu fault was the main reason of the great Assam earthquake (1950) of magnitude 8.7. The Shillong plateau tectonics have been associated with the great earthquake of 1897 of magnitude 8.1. The Shillong plateau region has witnessed mostly compressive tectonic forces in North-South, North East-South West and North West-South East directions. Region has four divisions (i) East-West trending zone consisting MBT and MCT (ii) Eastern syntax, (iii) Shillong massif & (iv) North-South trending features comprising of Arakam Yoma range & East boundary thrust. The East Himalayan zone is made up of Main Central Thrust (MCT), Main Boundary Thrust (MBT) and Main Frontal Thrust (MFT). Earthquake of greatest magnitude of 6.7 was occurred in this region on August 16, 1950. The Eastern syntaxis has MBT (Eastern region), MFT, Lohit thrust, Mishmi thrust, and Bame Tuting fault.

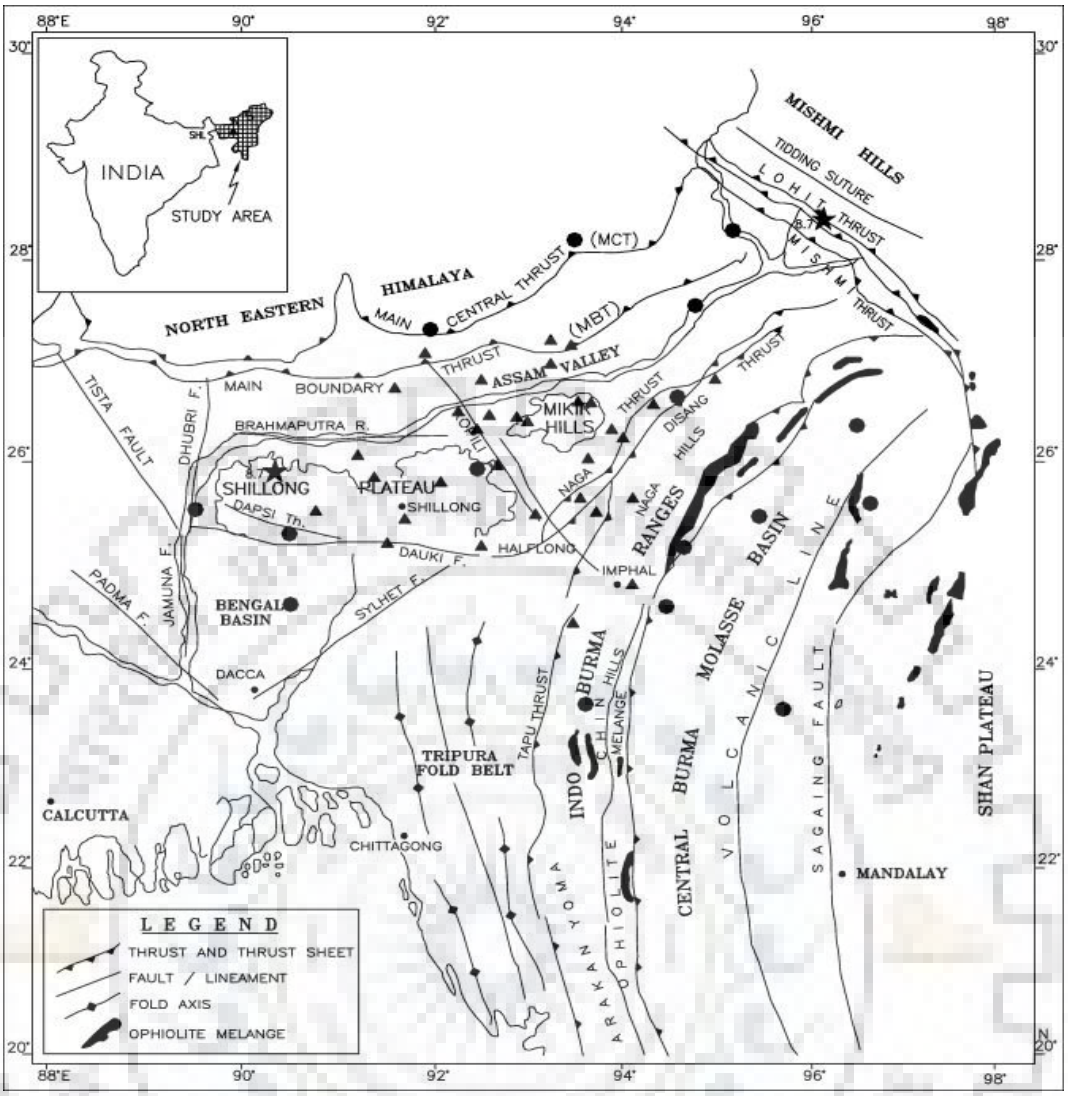

Figure 3.1 Tectonic features of the study area (Kayal, 1998)

Earthquake of greatest magnitude of 7.7 was occurred in this region on July 29, 1947. The Shillong massif has faults namely Dhansiri, Kopili, Dauki, Dudhnoi and Sylhet. Earthquake of greatest magnitude of 8.0 was occurred in this region on June 12, 1897. The N-S trending features has thrust zone of Naga-Disang, Eastern boundary thrust and Mat fault. Earthquake of greatest magnitude of 7.3 was occurred in this region on August 16, 1938 and March 21, 1954. South part of the Kopili fault is associated with the Cachar earthquake (1869) of M = 7.4. The India-Myanmar arc and Patkoi-Naga hills caused the Manipur earthquake (1988) of M = 7.2.

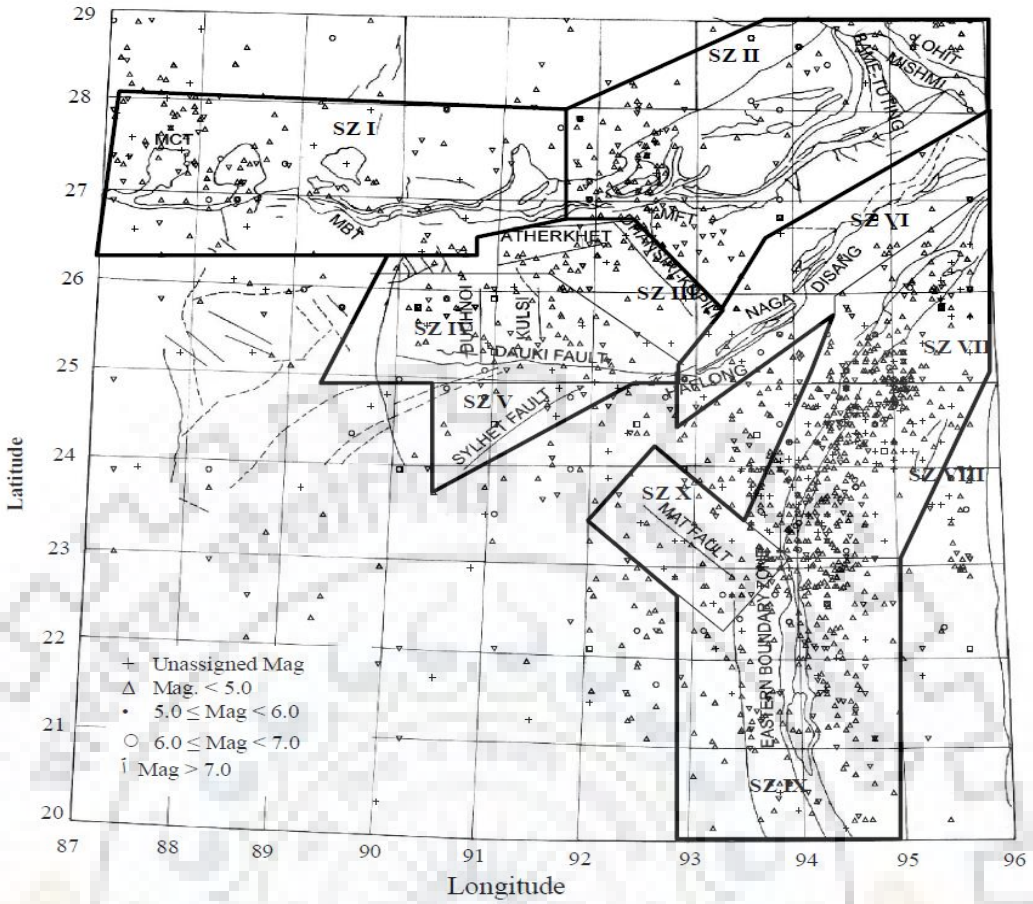

Figure 3.2 Seismotectonic map of the North-East Indian region with major zones and their subdivisions.(Sharma, 2006)

The north-east Indian region is divided into two geotectonic blocks by a geotectonic divide shown as line AB in Map. Number of earthquakes are located on the line striking between Shillong plateau and Mikir hills (Verma et. al. 1976). It has been found that epicenters of earthquakes in this region have increasing depth towards the Himalayas which shows the presence of a deep fault. Brahmaputra changes direction from NE-SW to EW direction from the line AB which can be presented as a geomorphological evidence for this.

Block - I It covers a part of Eastern Himalayas, Shillong plateau, western part of Brahmaputra valley, Surma valley, Tripura, a part of Mizoram and Manipur. The great Indian earthquake of 1897 occurred in this block.

Block - II It covers Arunachal Pradesh, eastern part of the Brahmaputra valley, a part of the Arakan-Yoma tectonic belts. The great earthquake of Assam (1950) happened in this block.

Chapter 4 ATTENUATION RELATIONSHIP

An attenuation relationship provides a functional relationship between a strong motion parameter such as ground acceleration, spectral response values, etc. and parameters which characterize earthquake, medium of propagation, geology of local site, structural parameters, etc.

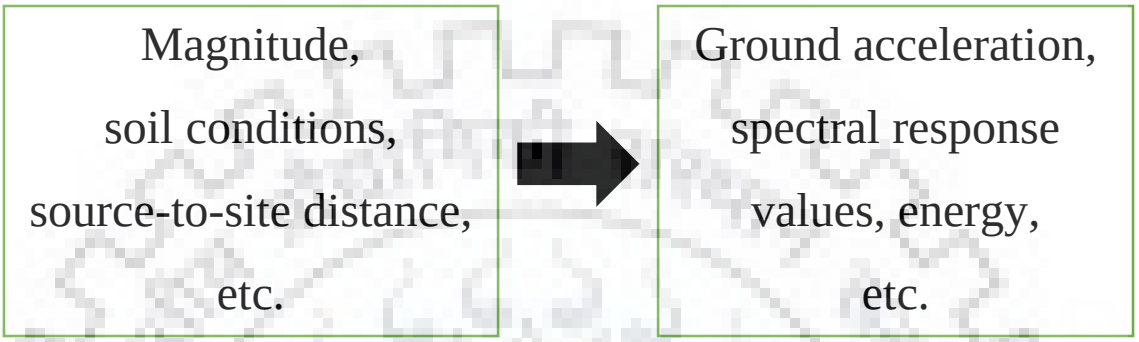

Figure 4.1 Simplified description of attenuation relationships

4.1 Factors affecting attenuation

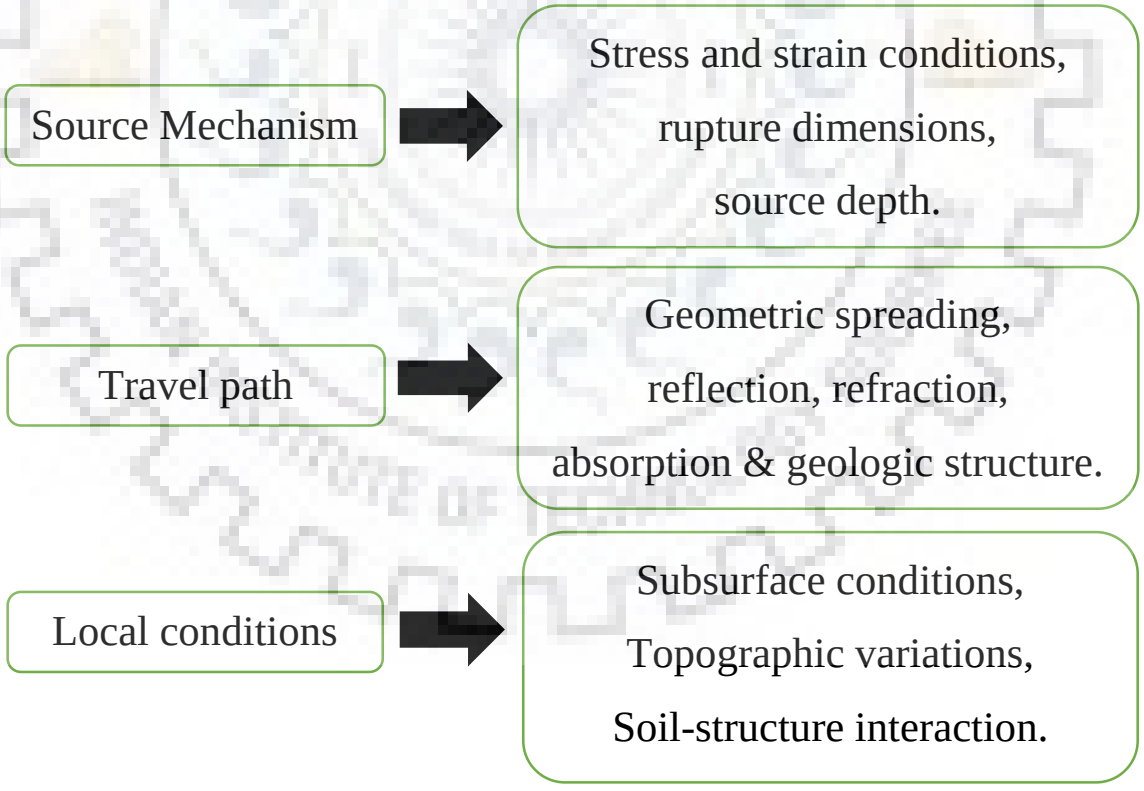

Figure 4.2 Simplified description of factors affecting attenuation

4.2 Types of attenuation relationships

Three main types of mathematical models were proposed in Draper & Smith (1981):

***Functional*:** In these a proper functional correlation exists between the value to be estimated & the predictor parameters are already known.

Control: In these the individual effects of each predictor parameter can be obtained with the help of predefined processes.

Predictive: When either of the above cannot be used and a heavy correlation exists within the data.

4.3 Strong ground motion parameters

These parameters describe the strong ground motions characteristics in a compact & quantitative form. Most of them characterizes the amplitude, frequency content & duration of strong ground motions.

4.3.1 Amplitude parameters

PGA: It is the largest absolute value of horizontal acceleration obtained from the accelerogram. This parameter is popularly used as strong ground motion parameter in attenuation relationships due to its pre-established correlation with forces of inertia, which are the biggest dynamic forces induced in structures. It can also be co-related to earthquake intensity. Peak vertical acceleration got less attention in earthquake engineering. For engineering purposes Peak Vertical Acceleration is assumed to be $2/3^{rd}$ of Peak Horizontal Acceleration.

Usually, ground motions with large PGA causes more destruction than small PGA, but not always. Although PGA is an important parameter but it does not provide information about the frequency content and duration of earthquake, thus presenting a need of supplementary information for the characterization of ground motion.

PGV: It can characterize ground motion at intermediate frequencies, more accurately because it is less sensitive to higher frequency. In many studies PGV is co-related to earthquake intensity.

PGD: However, it has an association with lower frequency component of the seismic motion, but because of errors in signal processing in the filtering of data and numerical

integration, it is difficult to be accurately determined. Thus it is rarely used as a parameter for exhibiting strong ground motion.

4.3.2 Other parameters

Energy: Energy released during any seismic event can also be measured and predicted to characterize the size of the event.

Arias Intensity: It is integral of the square of the acceleration–time history. It characterizes probable damageability.

Cumulative Absolute Velocity: It is an integral of the absolute acceleration time history. It is a parameter to indicate the probable structural damage. It is represented mathematically as:

$$\text{CAV} = \int_0^{t,max} |a(t)|dt \tag{4.1}$$

Pseudo Spectral Acceleration:

4.4 Earthquake parameters

Before modern instruments were developed, the earthquake sizes were described based on some qualitative description like intensity. As it may vary with people's perceptions and experience, therefore it is not a very reliable parameter in modern days which can be used in such attenuation relationships. Nowadays, modern seismographs allow us to describe earthquakes in quantitative aspects also like magnitude. Magnitude is an objective and quantitative measurement of an earthquake. Four major types of magnitude scales that are used are.

Richter Local Magnitude (M_L): It is defined as the logarithm of the maximum amplitude traced (in μm) recorded by Wood-Anderson seismometer which is placed at a distance of 100 km from the epicenter of the earthquake. It is the best known magnitude scale.

$$M_L = \log A - \log A_o(\Delta) \tag{4.2}$$

where A is maximum amplitude (in mm), Δ is epicentral distance (in km) and $A_o(\Delta)$ is maximum amplitude at Δ km for a standard earthquake. It has no lower or upper limit in the scale. This scale gets saturated at high levels.

Surface Wave Magnitude (M_S) : Surface wave magnitude is based on the amplitude of Rayleigh waves with a period of about 20 sec. It is expressed as:

$$M_S = log\ A + 1.66\ log\ \Delta + 2.0 \quad (4.3)$$

where A is maximum ground displacement (in μm) and Δ is epicentral distance of the seismometer measured in degrees.

Body Wave Magnitude (M_B) : It is based on some starting cycles of p-waves which are not strongly influenced by the focal depth. It is expressed as:

$$M_B = \log A - \log T + 0.01\ \Delta + 5.9 \quad (4.4)$$

where A is the p-wave amplitude (in μm) and T is the period of the p-wave (1 sec). It is also determined from the amplitude of one-sec-one-period of higher mode Rayleigh waves, which can be used to describe intraplate earthquakes.

Moment Magnitude (M_W) : For earthquakes of higher magnitudes, ground shaking becomes less sensitive to earthquake size. It is called as saturation. This scale is not subjected to saturation because it is based on seismic moment. It is expressed as:

$$M_W = (2/3) \log M_o - 10.7 \quad (4.5)$$

where M_o is the seismic moment in dyne-cm.

The scalar seismic moment is expressed as:

$$M_o = \mu AD \quad (4.6)$$

where μ is shear modulus of the material (in dyne/cm^2), A is the rupture area (in cm^2) and D is the average displacement on A (in cm).

Table 4.1 Comparison of different magnitude scales

Scale Type	Author	Size	Depth	Epicentral Distance (km)	Reference parameter	Applicable to area	Saturation
M_L	Richter (1935)	Small	Shallow	<600	Wave amplitude	Regional	Saturation occurs
M_B	Gutenberg & Richter (1956)	Small to medium	Deep	>1000	Wave amplitude (P-waves)	Worldwide	Saturation occurs
M_S	Gutenberg & Richter (1936)	Large	Shallow	>2000	Wave amplitude (LR-waves)	Worldwide	Saturation occurs
M_W	Kanamori (1977)	All	All	All	Seismic moment	Worldwide	N.A.

4.5 Propagation parameters

The distance travelled by the seismic waves from the source to the site is used in all the ground motion estimation relations to characterize the path. Joyner and Boore (1981) state that the distance from the origin of the actual seismic wave to the station should be used in attenuation relationships but this is difficult to determine for past earthquakes and impossible to predict for future earthquakes. Nowadays, many different types of this distance are being used, some of which are discussed below.

Epicentral Distance (d_e): It is the distance from the horizontal projection of the rupture's starting point on the earth's surface. It is very easy to measure as information of epicenter of all earthquakes is given.

Hypocentral Distance (d_h): It is the distance from the rupture's starting point. Although it is also reported for every earthquake but accurate estimation of focal depth of earthquake is difficult and heavily depends on the proper distribution of the recording stations (Gubbins, 1990). Since most of the earthquakes are shallow earthquakes (depth less than 30 km) d_e and d_h becomes almost equal.

Rupture Centroid Distance (d_c): It is the distance from the centroid of the rupture. For this dimensions of the rupture plane are required and then estimation of its centroid is done.

Centre-of-energy-release Distance (d_E): It is the distance from a point on the rupture plane where energy is considered to be concentrated. It is similar to rupture centroid distance.

Surface Projection Distance (d_f): It is also called Joyner-Boore or fault distance. It is the distance from the surface projection of the rupture plane of the fault. $d_f = 0$ for a point within the projection.

4.6 Site parameters

The local site conditions significantly affect the recorded strong ground motion at a particular accelerograph station. Therefore, serious efforts should be made to model the effect of the local site conditions on strong ground motion in the attenuation relationships. Failing to model this thing up will result in equations of very limited value, especially in cases when equations corresponds to intermediate and long-period spectral ordinates.

A technique is commonly used to incorporate site effects in ground motion prediction equations. In this multiplicative factors are assigned to different type of sites. This method was introduced by Trifunac in 1976. He considered three site conditions. Multiplicative factor used between basement rock and intermediate type rock was taken half of the multiplicative factor used between hard basement rock site and alluvium soil type site. This limited the generality of this method. Generally, we use the number of multiplicative factors one less than the number of site categories.

Sometimes due to inadequate data available about the site conditions, there comes difficulty in assigning multiplicative factors. In such cases, multiplicative factors from previous studies where similar site conditions prevail, have been taken. Earlier as well as recent studies have used binary classification of soil and rock. Generally, a site is categorized into soil (or alluvium) if the soil layer thickness is between 4 and 20 m since shallow soil layer does not affect the strong ground motion significantly. This has also been found that sites with shallow soil have higher ground motion in comparison to rock or stiff soil site and deep soil site have similar ground motion as rock. This is true for PGA, since it is a high frequency parameter and has no effect of local site conditions.

4.7 Structure parameters

We need some parameters which can characterize the effect of the structure, in which the recording was done, to do free-field predictions of strong ground motion. Ground motions are highly affected by the size and embedment of the structure housing the recording station. In a study Campbell (1979, 1983, 1984b) found that there was about 50% reduction in peak accelerations due to instrument embedment from ground level. In many studies (Crouse, 1976; Lee et. al., 1982) building embedment acts as an important factor controlling the short period ground motion reduction. Kinematic scattering due to very large and rigid foundations like that of nuclear power plants can cause significant reduction in the amplitudes when ground motion wavelength is smaller than foundation size. These effects will also vary with investigated strong motion parameter, source-to-site distance and earthquake size.

Response of the structure should also be considered while developing the strong motion attenuation relationship. Free field recordings can be amplified upto a great extent by small shelters in which instruments are placed especially when there is soft soil beneath.

Chapter 5 METHODOLOGY

5.1 Parameter selection

Parameter to be predicted is a strong motion parameter which is called as dependent variable. Parameters used to predict this variable are called as independent variables.

Two major considerations must be kept in mind while choosing the independent variable. First, this variable must characterize the earthquake, travel path, local site and the structure. Second, this variable should be easily predictable using the available data. The dependent variable must be selected so that it fulfils the purpose such as seismic zoning, mapping or designing.

In this study PGA is selected as dependent variable of the equation since it is commonly used and very well characterize the source, path and site effects. Also the acceleration time history is easily available and can be used without much processing. Acceleration time history incorporates both time and frequency features of ground motions. Response spectrum can also comprehensively describe the ground motion but they are not readily available and large number of attenuation relations are required, for every structural period and damping, to predict the required response spectra.

Strong motion data are collected on three orthogonal components i.e. two horizontal and one vertical. This study is about horizontal strong ground motions. The two horizontal components can be used after treatment in some of the following ways:

1. taking largest of the two components,
2. taking both components,
3. taking mean of both components,
4. taking vectoral combination of both components,
5. random selection of components.

In this study, treatment number 1, 2, 3 and 4 are used so that a comparative analysis between them can be done to extract out the best suitable equation.

While using both horizontal components, the resulting prediction will represent a random selection of the orientations of the components. This will give median predictions which will be identical to those obtained by using the mean of the two, but the standard deviation

will be larger in the former case (Campbell, 1982a). There exists a strong correlation among the two horizontal components and thus using these two as two different independent data points will enhance the statistical significance of the analyses in an artificial manner. This can be avoided if their mutual dependence is properly addressed in the analyses.

5.2 Earthquake parameters used

Magnitude is the most common term used in attenuation relations to characterize earthquake size. Magnitude is regularly informed by seismographic station networks for each seismic event regardless of its size. Many other source parameters were used in past studies like source dimensions (Ts'ao, 1980; Bernreuter, 1981b), seismic moment or moment magnitude (Hanks, 1979; Hanks and McGuire, 1980, 1981; Joyner and Boore, 1981, 1982; McGuire et. al., 1984), and stress drop (Hanks and Johnson, 1976; Hanks, 1979; Ts'ao, 1980; Bernreuter, 1981b; Hanks and McGuire, 1980, 1981; McGuire et. al., 1984).

Stress drop estimation has a very high degree of uncertainty. Calculation of seismic moment for past earthquakes is mostly unavailable. Hence, earthquake magnitude is the easiest and most reliable parameter to characterize the earthquake and it is reported for every event since a long time. But as we know there are a variety of magnitude scales existing, this can lead to confusion as to which is to be used when. Also it will be difficult to compare different attenuation relationships using different scales. Also we know that all scales saturate at higher magnitudes except moment magnitude scale. Most magnitude scales are based on peak amplitude of seismogram, there exist a strong correlation between magnitude and ground motion parameter. Boore in 1980 found a strong correlation between peak velocity and local magnitude. M_b (body wave magnitude) and M_L (local magnitude) might correlate with high frequency ground motion and M_S (surface wave magnitude) and M_W moment magnitude) might correlate with low frequency ground motion.

Typically, M_b or M_L are used for smaller earthquakes and M_S or M_W for larger earthquakes. Richter scale developed by Nuttli (1979) suggests M_L for magnitude less than about 6 and M_S for larger earthquakes. In this study, the earthquake magnitudes reported by seismographic station network are in Richter scale. Magnitude range taken is 3.7 to 6.8 in the present study.

5.3 Propagation parameters used

These parameters characterize the effects of scattering of seismic waves, geometrical attenuation and anelastic attenuation of ground motion as the wave travels from the source to the site. Distance is the independent variable used to characterize these parameters universally. Nowadays, a number of distance measures are being used. For sites which are located at a distance which is very large in comparison to source dimensions, there is not much difference between distance measures. Predictions in near source regions are of ultimate concern.

In this study hypocentral distance is used for all the records. The hypocentral distance for the earthquake records varies from 19.35 km to 288.73 km. A filtering of depth equal to 100 km has been applied. By using hypocentral distance we have already taken into account the focal depth of each earthquake event. This hypocentral distances are calculated from the available information about the latitudes and longitudes of the earthquake event source and recording stations.

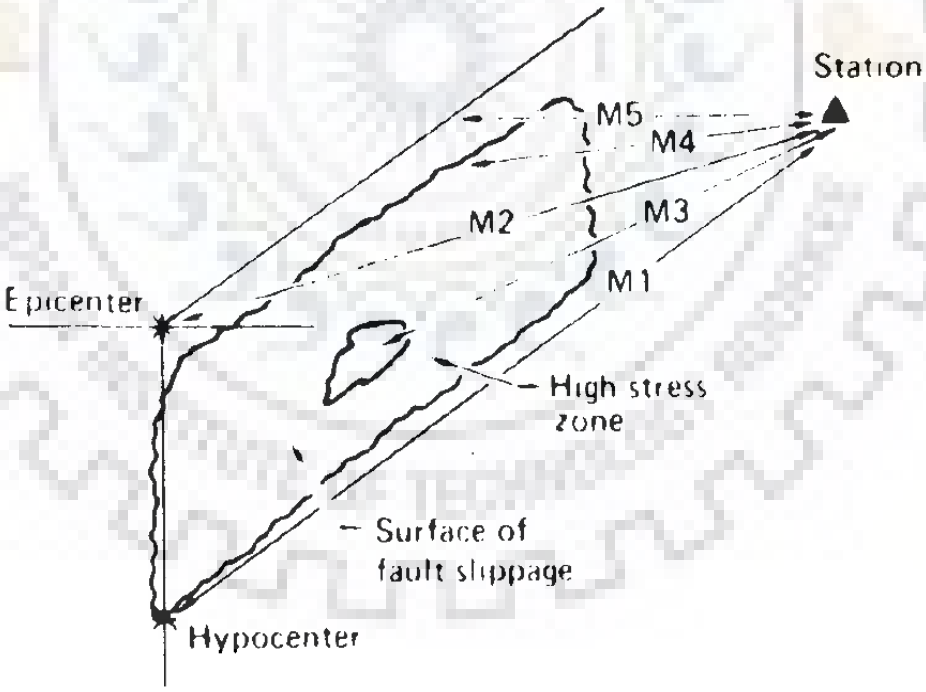

Figure 5.1 Distance measures used in strong motion attenuation relationships: M1 (hypocentral distance); M2 (epicentral distance); M3 (distance to energetic zone); M4 (closest distance to rupture zone); M5 (closest distance to surface projection of rupture zone). (Campbell, 1985)

Table 5.1 Description of different distance measures

Distance Definition	**Distance Measure**	**Examples of Attenuation Relations Using the Distance Measure**
Shortest horizontal distance to the vertical projection of the rupture	"Joyner-Boore" distance	Joyner & Boore (1981), Boore et. al. (1997), Spudich et. al. (1996).
Closest distance to the rupture surface	Rupture distance	Sadigh et. al. (1997), Idriss (1995), Abrahamson and Silva (1997).
Closest distance to the seismogenic part of the rupture	Seismogenic distance	Campbell (1997).
Closest distance to the hypocenter	Hypocentral distance	Atkinson and Boore (1995).
Closest distance to the centroid	Centroid distance	Crouse (1991).

5.4 Site parameters used

Site parameters are related to geological conditions around the recording stations. As we know from a numerous studies that local site geology and soil conditions plays a significant role in the strong ground motions, it is very much required to take parameters pertaining to these local conditions so as to properly address them and obtain their effect on the estimated ground motion through the attenuation relationship. In some studies, site parameters used is wave propagation velocity.

There are some major factors to be considered while selecting these parameters. First is the complex relationship which exists between site and structure effects. Other factors like fault mechanism, site topography, soil depth, instrument embedment and structure size affect the quantification of site effects significantly. Many studies observed a large amplification for shallow soil deposits sites located near source of small to moderate earthquakes. This can sometimes reach upto a factor of two.

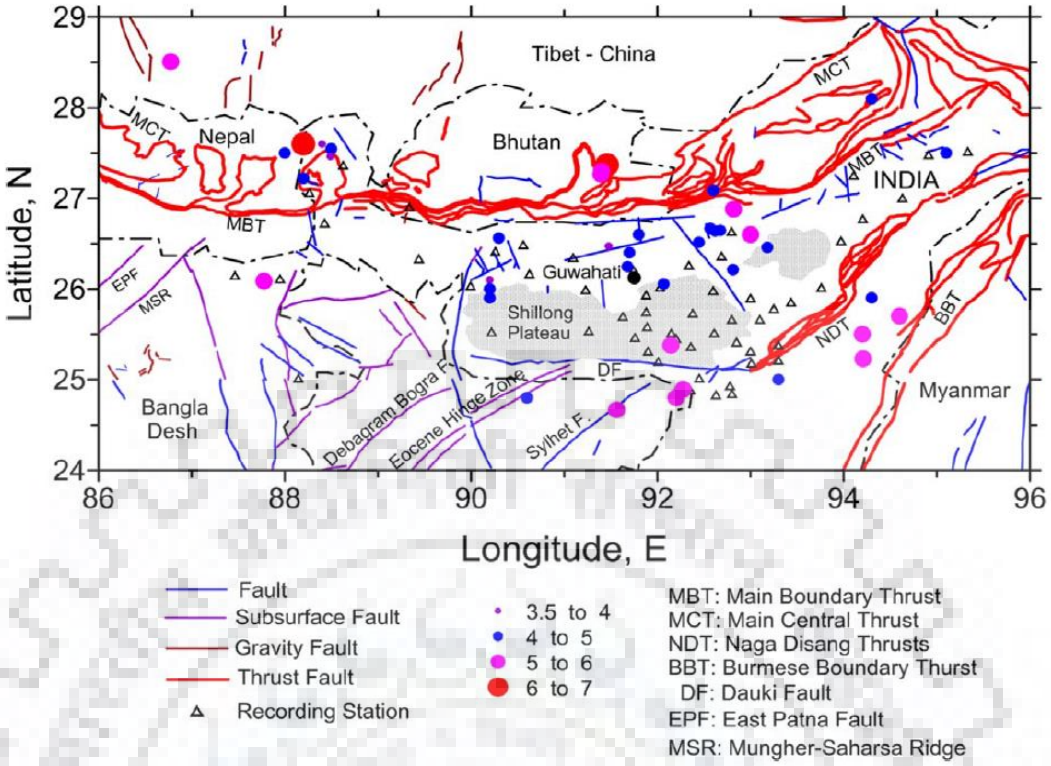

Figure 5.2 North-East Indian region map with locations of recording stations and epicenters of contributing earthquakes. (I.D. Gupta & M.D. Trifunac, 2017)

Site parameters for local geology and soil conditions have been assigned to all the recording stations from which the database has been prepared. In this study, the site classification done for local geology is same as done by Trifunac and Brady (1975). A parameter s has been adopted and is assigned values from 0 to 2 for three site geology categories. 0 to 2 values represent these three categories in increasing order of "hardness". The class denoted by s = 0 represents the stations located on sedimentary deposits. The class denoted by s = 1 represents the stations located on intermediate rocks and complex geological environments which are difficult to put in class s = 0 and s = 2. The class denoted by s = 2 represents the stations located on basement rocks. 84.25% i.e. 214 out of 254 accelerograms represent deep sediments site, while only 3.94% i.e. 10 out of 254 accelerograms represent intermediate rock sites and only 11.81% i.e. 30 out of 254 accelerograms represent basement rock sites. These stats show that the distribution is skewed for the North-East Indian region. An important consideration which should be kept in mind is that site classification scheme which is selected must be compatible with the strong ground motion parameter which is to be predicted through the attenuation relationship.

Table 5.2 Details of the recording stations used for the present database.

Sr. No.	Station		Location		s	Geology in brief
	Name	Code	Latitude	Longitude		
1.	Araria	ARI	26.134	87.466	0	Quaternary Alluvium
2.	Barpeta	BAR	26.332	91.096	0	Quaternary Alluvium
3.	Boko	BOK	25.976	91.230	0	Quaternary Alluvium
4.	Bongaigaon	BON	26.473	90.561	0	Quaternary Alluvium
5.	Koochvihar	COB	26.319	89.440	0	Quaternary Alluvium
6.	Dhubri	DHU	26.020	89.995	0	Quaternary Alluvium
7.	Dibrugarh	DIB	27.467	94.912	0	Quaternary Alluvium
8.	Diphu	DIP	25.839	93.435	0	Quaternary Alluvium
9.	Darjeeling	DJL	27.050	88.265	2	Gneissic Complex
10.	Goalpara	GLP	26.152	90.627	0	Quaternary Alluvium
11.	Golaghat	GOL	26.516	93.972	0	Quaternary Alluvium
12.	Gangtok	GTK	27.352	88.627	2	Gneissic Complex
13.	Guwahati	GUA	26.190	91.746	0	Quaternary Alluvium
14.	Jorhat	JHR	26.759	94.206	0	Quaternary Alluvium
15.	Karimganj	KAR	24.870	92.354	0	Quaternary Alluvium
16.	Kokrajhar	KOK	26.400	90.261	0	Quaternary Alluvium
17.	Kishanganj	KSN	26.097	87.950	0	Quaternary Alluvium
18.	North Lakhimpur	LKH	27.239	94.107	0	Quaternary Alluvium
19.	Malda	MLD	25.000	88.146	1	Quaternary Alluvium
20.	Mangaldai	MNG	26.003	92.029	0	Quaternary Alluvium
21.	Morigaon	MOR	26.248	92.339	0	Quaternary Alluvium
22.	Naogaon	NAU	26.349	92.690	0	Quaternary Alluvium
23.	Nongstoin	NON	25.522	91.264	2	Gneissic Complex
24.	Sibsgar	SBS	26.989	94.631	2	Gneissic Complex
25.	Silchar	SIL	24.830	92.801	0	Quaternary Alluvium
26.	Siliguri	SLG	26.712	88.428	0	Quaternary Alluvium
27.	Tinsukia	TIN	27.503	95.332	0	Quaternary Alluvium
28.	Tura	TUR	25.511	90.220	1	Sandstones
29.	Tejpur	TZP	26.619	92.797	0	Quaternary Alluvium

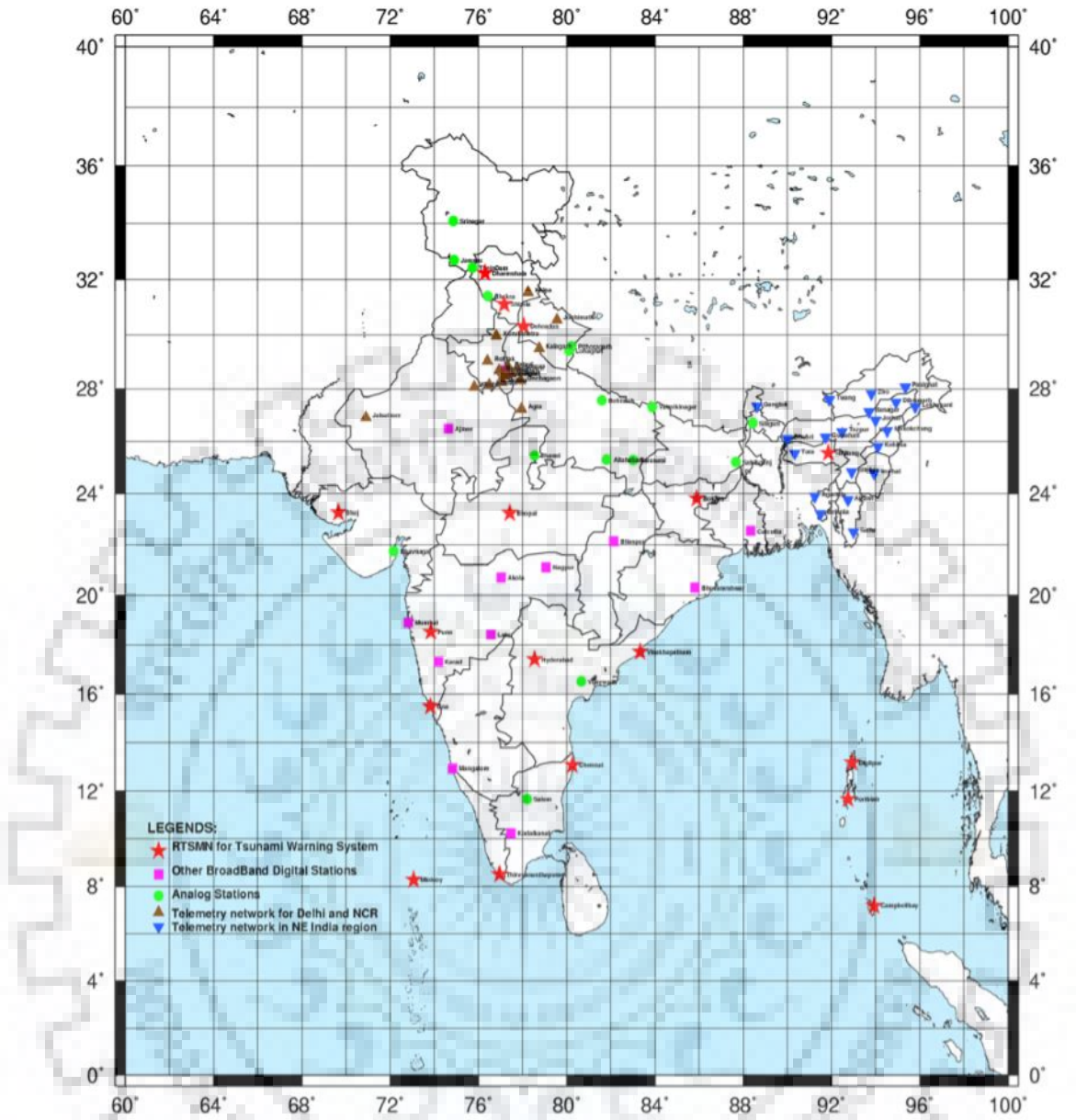

Figure 5.3 Seismic recording stations map of India. (Google images)

5.5 Data selection

After selecting dependent and independent parameters, a database is prepared. A database should be prepared which fulfils minimum standard of quality and should also be consistent. From the beginning one must take serious precautions and care to attain these benchmarks. If, somehow, these conditions are not fulfilled, there will be biases in the analyses. These biases will increase tremendously, scatter in the predictions. Thus the reliability of the obtained equation will be totally lost. One can largely avoid these biases and scattering by simply selecting the records so that they represent (i) tectonic area of similar attenuation and source characteristics, (ii) recording instruments of similar

response characteristics, (iii) consistent and accurate record processing techniques, and (iv) consistent definitions of strong motion, earthquake, path, site and structure parameters. Data selected should have a range of each parameter used so that the prediction can be as accurate as possible. Data used outside of this range can again cause biases and scattering in predictions. Also if independent parameters are statistically correlated then there will be biasing in the prediction of the coefficients during regression analysis. Scatter plot (Fig 5.4) can be used to observe any existing correlation. Selection criteria can be modified or special techniques of analyses can be if large biases are found. Various processing techniques are to be employed so that the raw data can be suitably used in regression. Segregation, filtering, homogenization, sorting, ordering, etc. are few of these processes which are done over the obtained data. Various tables and sheets are made for the regression analyses to be done.

A consistent data can be obtained by (i) excluding the records which does not have the recording characteristics which are to be predicted, and (ii) including parameters which address these characteristics adequately. When unwanted recordings are there in a small percentage of the total data set we can ignore it by using first technique. When there is insufficient data required for a stable statistical analyses then second technique is used.
If the data represent a systematic characteristic of the earthquake, path, site or structure then the predicted strong motion will have large uncertainty. Also a random characteristic (which cannot be reliably predicted in future) should not be removed from the database.

In this present study, the data has been obtained from www.pesmos.in, a website of IIT Roorkee. Earlier in 1970s, the Department of Earthquake Engineering at the then University of Roorkee (currently IIT Roorkee) developed and deployed RESA (Roorkee Earthquake School Accelerograph) series to record strong ground motions. But it failed to record any strong ground motion. 147 three component records 0f 13 earthquakes has been recently available for the period of 1986-1999. These records were obtained from 135 state-of-the-art analog accelerographs (SMA-1 manufactured by Kinemetrics). They were located in Garhwal-Kumaon and Kangra region of western Himalayas and Shillong Plateaus of north-east India. Department of Science and Technology (DST), New Delhi also supported these networks. During 2005, a network of 300 modern digital accelerographs was installed by these two organizations in vast areas of western Himalayas, northeast India and Indo-Gangetic alluvial plains. It was called “National

Strong Motion Instrumentation Network". Data of 485 three component accelerograms from 144 earthquakes occurred during 2005-2014 is available PESMOS website which is under IIT Roorkee. The present database comprises of 52 different earthquakes from the period of 2008-2014.

Table 5.3 Description of earthquakes considered in this study.

Sr. No.	Date	Magnitude	Latitude	Longitude
1.	27/03/2012	4.9	26.1 N	87.8 E
2.	15/02/2009	4.4	26.0 N	90.2 E
3.	02/03/2013	5.2	24.8 N	92.2 E
4.	16/04/2013	4.6	26.3 N	92.0 E
5.	06/11/2013	5.5	26.5 N	93.5 E
6.	30/05/2014	4.5	26.5 N	90.4 E
7.	12/09/2014	4.2	26.1 N	90.2 E
8.	25/04/2009	4.0	26.4 N	91.7 E
9.	11/08/2009	5.6	24.4 N	94.8 E
10.	19/08/2009	4.9	26.6 N	92.5 E
11.	30/08/2009	5.3	25.4 N	94.8 E
12.	03/09/2009	5.9	24.3 N	94.6 E
13.	21/09/2009	6.2	27.3 N	91.5 E
14.	26/07/2008	4.8	24.8 N	90.6 E
15.	15/02/2009	4.4	26.0 N	90.2 E
16.	29/10/2009	4.2	26.6 N	90.0 E
17.	29/10/2009	5.2	27.3 N	91.4 E
18.	31/12/2009	5.5	27.3 N	91.4 E
19.	11/09/2010	5.0	25.9 N	90.2 E
20.	18/09/2011	6.8	27.6 N	88.2 E
21.	18/09/2011	5.0	27.6 N	88.5 E
22.	24/02/2009	4.8	25.9 N	94.3 E
23.	26/02/2010	5.4	28.5 N	86.7 E
24.	03/06/2011	4.9	27.5 N	88.0 E
25.	30/11/2012	4.1	27.3 N	88.3 E
26.	11/05/2012	5.4	26.6 N	93.0 E

27.	01/07/2012	5.8	25.7 N	94.6 E
28.	14/07/2012	5.5	25.5 N	94.2 E
29.	02/10/2012	5.1	26.9 N	92.8 E
30.	09/01/2013	5.9	25.4 N	94.9 E
31.	25/12/2008	4.4	27.2 N	87.9 E
32.	18/09/2011	4.5	27.6 N	88.4 E
33.	18/09/2011	4.2	27.6 N	88.4 E
34.	22/09/2011	3.9	27.6 N	88.4 E
35.	26/07/2010	4.1	26.5 N	91.3 E
36.	04/02/2011	6.4	24.8 N	94.6 E
37.	12/12/2010	4.8	25.0 N	93.3 E
38.	04/05/2012	4.4	27.5 N	95.1 E
39.	13/03/2008	4.0	26.6 N	91.8 E
40.	29/05/2008	4.2	26.6 N	91.8 E
41.	10/07/2012	4.5	26.5 N	93.2 E
42.	30/10/2012	3.9	26.2 N	92.4 E
43.	21/08/2013	3.9	26.7 N	92.4 E
44.	07/10/2013	3.7	26.3 N	92.5 E
45.	23/02/2014	4.8	27.2 N	92.5 E
46.	01/04/2014	4.4	26.4 N	92.4 E
47.	07/07/2008	5.1	26.1 N	95.1 E
48.	07/01/2013	4.5	28.1 N	94.3 E
49.	19/08/2012	5.0	26.7 N	92.5 E
50.	19/08/2012	4.0	26.7 N	92.5 E
51.	21/08/2013	4.2	26.7 N	92.5 E
52.	21/08/2013	3.9	26.7 N	92.5 E

Figure 5.4 represent the distribution of taken data. Distribution of taken data with respect to magnitude and hypocentral distance shows that we have a uniformly distributed data with lower magnitudes recorded at lower distances and higher magnitudes recorded at higher distances. Distribution of PGA values for both the components with respect to hypocentral distance show that the distribution is uniform for a range of PGA values and range of hypocentral distance too.

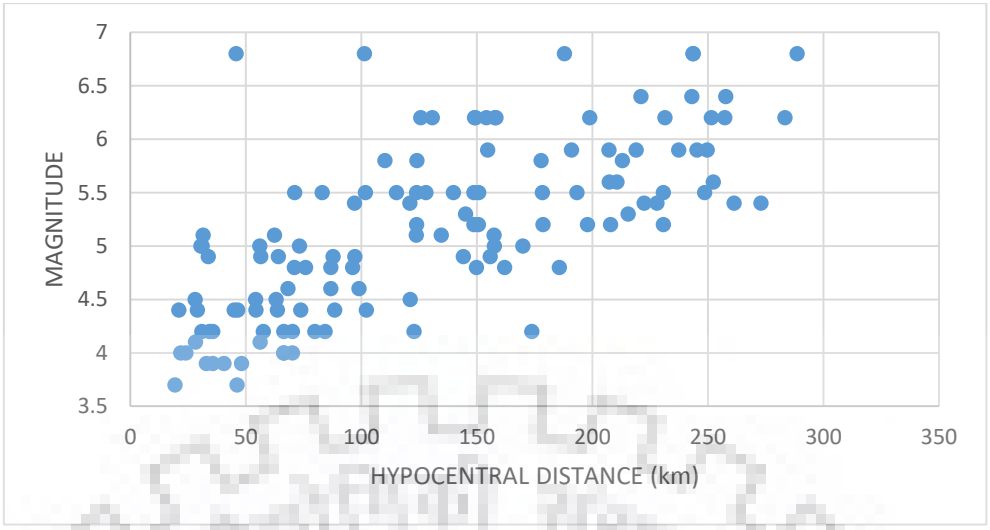

(a)

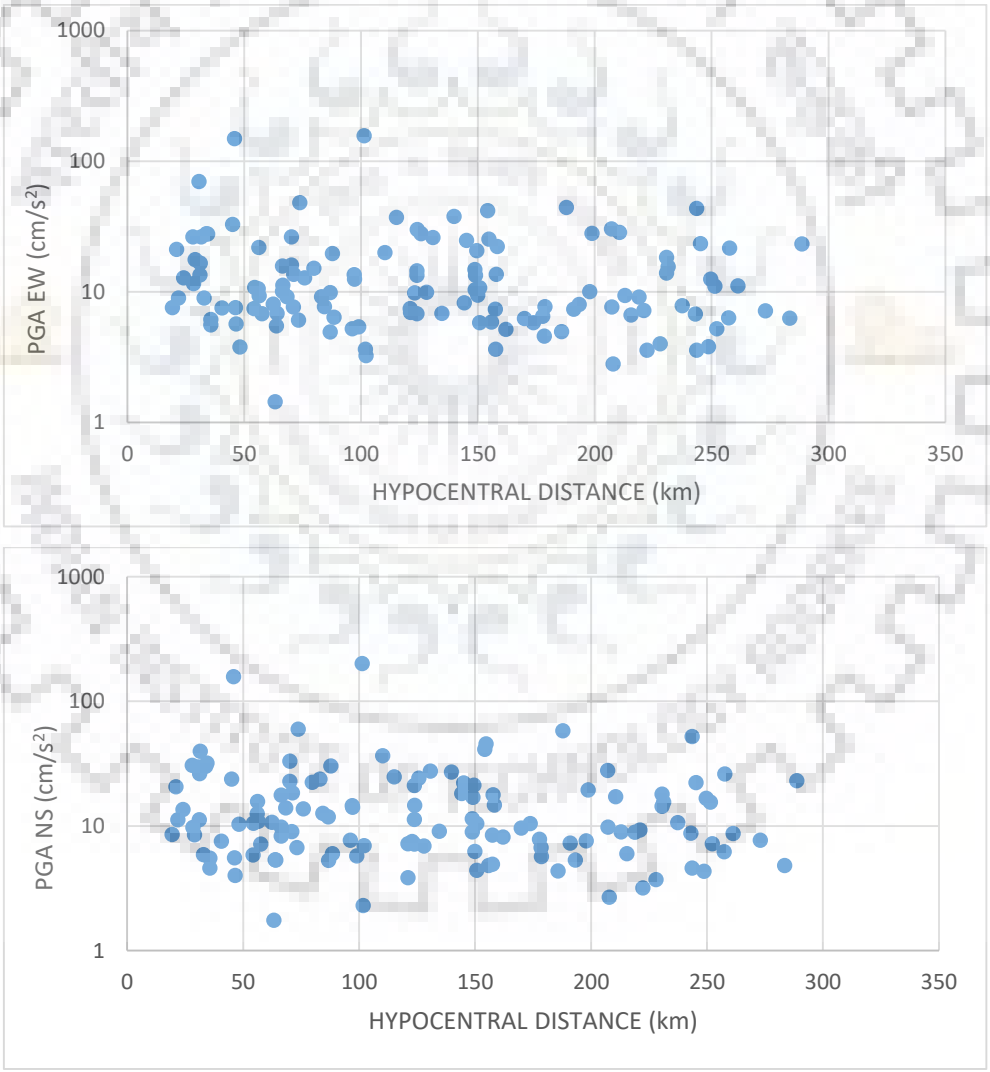

(b)

Figure 5.4 Distribution of taken data. (a) Distribution of taken data with respect to magnitude and hypocentral distance. (b) Distribution of PGA values for EW and NS components with hypocentral distance.

5.6 Ground motion attenuation model

5.6.1 Introduction

Earthquakes causes ground shaking which causes damage to structures. But this shaking attenuates with increasing distance from the source. To obtain the attenuation relation which properly address the effects of earthquake size, distance from source and various geological characteristics, on the required ground motion intensity measures such as peak ground acceleration, we need a predictive model which, after regression analyses of the data, gives us the required equation.

Generally, for designing of the engineering structures, ground motions are estimated either by using building codes or in site specific design of structures. Ground motion recordings for a specific site are rarely available in sufficient numbers so that empirical relation can be derived for the ground motion for a design earthquake. These type of relationships are required, for at least a large area or area of a specific tectonic feature. These can be applied in site specific design and regional hazard mapping.

5.6.2 Attenuation model

Selecting a suitable model for the attenuation relationships is a very important step. A suitable model implies that all the parameters should be properly addressed in it. Following are some rules for selecting model:

1. standard deviation of the resulting equation should be as low as possible,
2. attenuation model should have physical and practical background,
3. predicted results should be able to be applied to areas which are in lack of strong ground motion records.

5.6.3 Attenuation mechanism

Our earth is not a perfect transmitter of seismic energy. With the increasing distance from the source, the energy will be lost. Earth is not elastic material, therefore anelastic losses occurs as the seismic wave propagates through the earth. This anelastic behavior causes dispersion, affects the pulse shape and the amplitudes of the waves.

Attenuation effects can be categorized into two categories. First is intrinsic anelasticity in which crystal dislocations, friction and relative movement of the fluids located in the

interstices are covered. Second one is scattering attenuation which covers redistribution of seismic wave energy by reflection, refraction and interaction with the irregularities found in the medium. Geometrical spreading is also a major cause of attenuation. Earth is made up of complex material and hence attenuation process is also a very complex mechanism. For this a simple model which can simulate the attenuation properly should be selected.

5.7 Predictive equation

These equations represent ground motion as a functional form of earthquake size and geological parameters. Functional form minimizes the number of empirical coefficients and enhances the reliability of the equation. The common functional form can be chosen according to the following observations.

1. Peak ground motion values are observed to be approximately lognormally distributed. Therefore, the regression analyses are done on the logarithmic of the predictive term instead of the term itself.
2. Earthquake magnitude is defined typically as the logarithm of some peak motion parameters. Thus the magnitude is approximately proportional to the logarithm of peak ground motion values.
3. Body wave amplitudes are inversely proportional to the distance from the source and surface wave amplitudes are inversely proportional to the square root of the distance from the source. And seismic energy is directly proportional to the square of wave amplitude.
4. Fault rupture area is proportional to the earthquake magnitude. Thus, some waves producing strong motion at the specific site arrives from small distances and some from large distances. The effective distance is greater than the small distances. Therefore, distance scale should be properly selected.
5. Material damping and anelasticity of the material through which the waves travel are also considered.

Combining all the above considerations and observations, the predictive attenuation equations are discussed below.

The general functional form of the equation from some previous works can be expressed as:

$$f(Y) = a + f_1(M) + f_2(R) + f_3(S) + \varepsilon \quad (5.1)$$

where Y is the ground motion parameter to be predicted, like PGA, PGV, Arias intensity, etc.

$f_1(M)$ is a function of magnitude, $f_2(R)$ is a function of distance, $f_3(S)$ is a function taken into account of the site categories and ε is a value representing the uncertainty in the predicted $f(Y)$. No coupled terms of these variables are taken into account.

The forms of $f(Y)$ and $f_1(M)$ are selected as:

$$f(Y) = \log_{10}(Y) \tag{5.2}$$

$$f_1(M) = bM + cM^2 \tag{5.3}$$

Geometrical spreading, material anelasticity and scattering effect can be accounted in the function $f_2(R)$ and it can be expressed as:

$$f_2(R) = d \log_{10}(R^2 + h^2)^{0.5} + eR \tag{5.4}$$

where the first term represents the geometrical spreading and the second term represents the anelastic attenuation. Parameter h is called as 'fictitious depth' and in the present study it is accounted by taking hypocentral distance. h is determined by regression and it incorporates all the factors due to which the motions are limited near the source which is called saturation with distance [Joyner and Boore, 1981; Campbell, 1985]. h value incorporates all those factors that tends to limit or reduce the motions near the source [Ambraseys, 1974]. It also incorporates any factor which tends to enhance the motion near the source in a particular directivity [Boore and Joyner, 1978].

According to Joyner and Boore (1993), the inelastic attenuation coefficient e was not found to be statically significant and has a value almost equal to zero. Therefore, this term being negligible can be ignored in the equation.

Functional form of $f_3(S)$ can be expressed as:

$$f_3(S) = f S \tag{5.5}$$

where f is a regression coefficient and S represent site categories, 0 for sedimentary deposits, 1 for intermediate rocks and other complex geological environments which are hard to put in class S=0 and S=2 and 2 for basement rocks. The other details of these site categories have been discussed earlier.

According to the above discussion the final functional form for modelling the ground motion attenuation can be expressed as:

$$\log_{10}(Y) = a + bM + cM^2 + d \log_{10}(R^2 + h^2)^{0.5} + f S \pm \sigma \tag{5.6}$$

where σ is the standard deviation of the logarithm of Y, M is the magnitude and the whole term $(R^2 + h^2)^{0.5}$ is replaced by R_{HYPO} representing hypocentral distance.

In order to determine the coefficients and standard deviation σ, a two-step regression analysis as used by [Joyner and Boore, 1981], has been used in the present study.

5.8 Two-step regression method

Many methods have been proposed to obtain the attenuation relationship. Two commonly used regression methods which correlate the ground motion data are: two-step regression method and random effects method. In this study, two step regression method has been employed which was proposed by Joyner and Boore (1981). In the first step, distance and site condition dependence was determined along with a set of factors for each earthquake magnitude. In second step, these factors were regressed against the magnitudes to determine magnitude dependence.

In two-step regression method, ground motions are fit to a model in which each earthquake has a constant a_i, thus the attenuation model is:

$$\log_{10}(Y_{ij}) = g_1(R_{ij}, S_{ij}, \ldots\ldots) + \sum_{k=1}^{n} E_{ik}\, a_i \qquad (5.7)$$

where Y_{ij} is the ground motion parameter (peak ground acceleration in this study) from the j^{th} recording and i^{th} earthquake. n is the number of earthquakes (52 in this study). E_{ik} is a dummy variable equals to 1 if $i=k$ and 0 otherwise. $g_1(R_{ij}, S_{ij}, \ldots\ldots)$ is a function of distance, magnitude and site category. a_i are intra-event terms depending on the earthquake scenario.

In the second regression step, the event terms are then regressed and fit to a model representing magnitude dependence. Objective of this step is to capture the intra-event parameters a_i.

$$a_i = g_2(Magnitude) \qquad (5.8)$$

The advantage of this method is that the data from each earthquake is generally recorded over a limited range of distance, hence errors in measuring magnitude does not affect the distance coefficient obtained after the regression. Another advantage is that it causes each earthquake to have the same weight in determining magnitude dependence and each recording to have the same weight in determining distance dependence, which intuitively seems appropriate. But Joyner and Boore suggest using weights in the two-step regression method [Joyner and Boore, 1993].

Chapter 6 DATA ANALYSIS & VALIDATION

Earthquake resistant structures require the estimation of ground motion to which they will be exposed. Level of shaking is best described by ground motion parameters such as peak ground acceleration or response spectral ordinates. These relationships play a significant role in seismic hazard analysis and seismic design of structures. This chapter deals with the searching and processing of the strong ground motion data and how the final equation is obtained.

The whole research in this field is based on the fact that how much data is available for the past earthquakes both in a quantitative and qualitative aspect. The three basic steps to determine the attenuation relationship are:

1. Selection of a proper functional form which describe magnitude dependence, decay with increasing distance and the effects of site conditions on the ground motions.
2. Selection of database and the number of available data and its distribution will affect the robustness and reliability of the predicted value.
3. Selection of regression analysis to obtain the coefficients of the equation to fit the data.

The database in this study is prepared from the data obtained from the website of www.pesmos.com of IIT Roorkee Earthquake Engineering Department. This database covers 127 recordings, each having N-S and E-W horizontal components of 52 earthquakes from the period of 2008 to 2014 occurred in North-East Indian Region. The region covered is from 24.3^0 N to 28.5^0 N and from 86.7^0 E to 95.1^0 E. the magnitude range covered is from 3.7 to 6.8. Hypocentral distance is upto 300 km.

In this study, a comparative analysis has been done between the equations obtained after considering the following four conditions:

1. Taking both horizontal components of each recording.
2. Taking the maximum of the two horizontal components of each recording.
3. Taking the mean of the two horizontal components of each recording.
4. Taking the square root of sum of squares (SRSS) of the two horizontal components of each recording.

6.1 Taking both horizontal components

Considering both the horizontal components for the regression analysis gives larger database i.e. twice the size as compared to other cases. In first step of the regression analysis, the intercept is fixed to zero value. But in second step, intercept is not fixed. In the second step, the coefficient of M^2 was obtained as a positive value, therefore second step was again done without considering the term M^2. After both steps the final equation obtained can be expressed as:

$$\log_{10}(PGA) = 0.88586 + 0.39807\,M - 0.93413\log_{10}(R_{HYPO}) - 0.01057\,S \pm 0.21787 \quad (6.1)$$

where PGA is peak ground acceleration in cm/s^2. The standard deviation for the predicted result is 0.21787.

The following graph is showing the attenuation curves of the predicted values with hypocentral distance for magnitudes 5, 6, 7 and 8 and for soil and rock site categories. The PGA axis is in logarithmic scale and unit is cm/s^2. While the hypocentral axis is in normal scale and unit is in km.

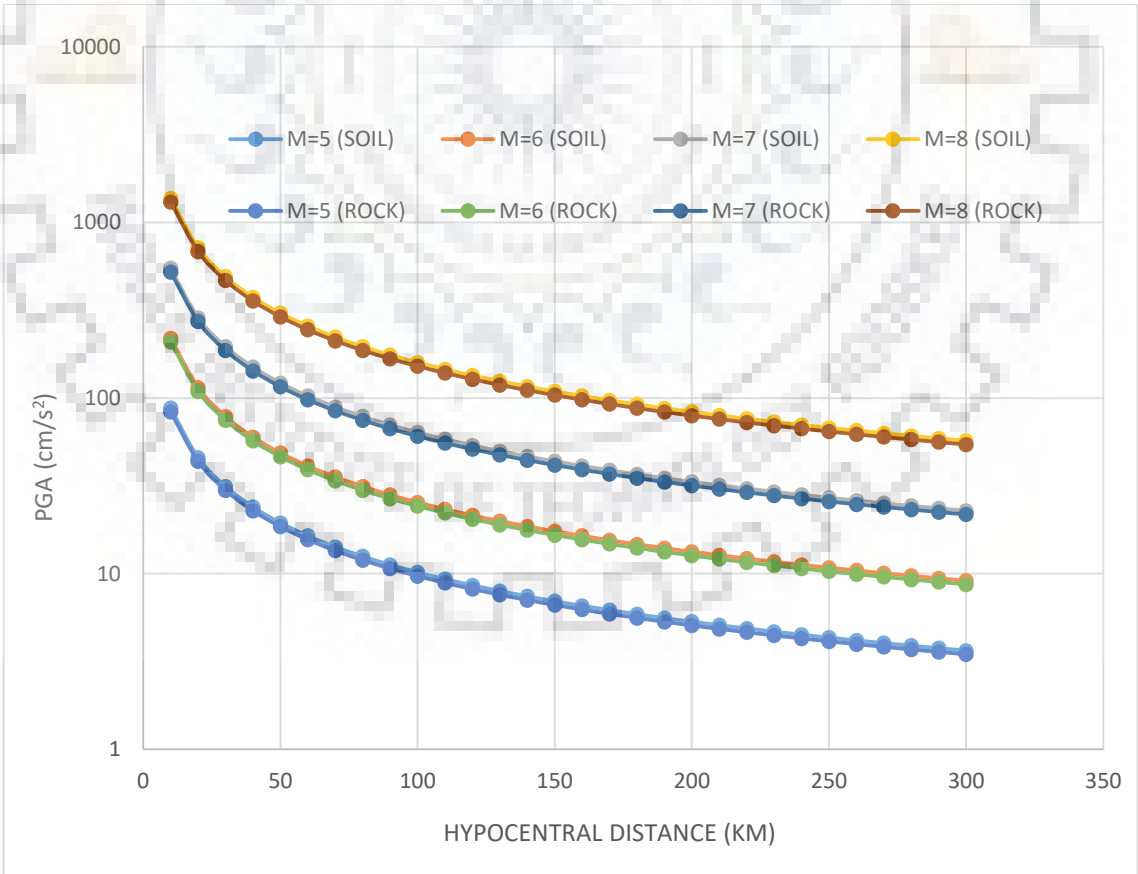

Figure 6.1 Predicted horizontal PGA attenuation curves by equation (6.1) with respect to hypocentral distance for magnitudes (M = 5.0; 6.0; 7.0; 8.0) for soil and rock sites.

From the above figure, it can be easily observed that PGA values for soil site category is always greater than rock site category for given conditions. This is because of the amplification effect of local site conditions. But this difference in values is very small because only 4 stations out of 29 are located on basement rock sites. This is reflected in the results of the regression analysis. The coefficient of site category obtained is quite small and is equal to 0.01057. Also the shapes of the curves are independent of the magnitude, showing that the distance decay is independent of magnitude.

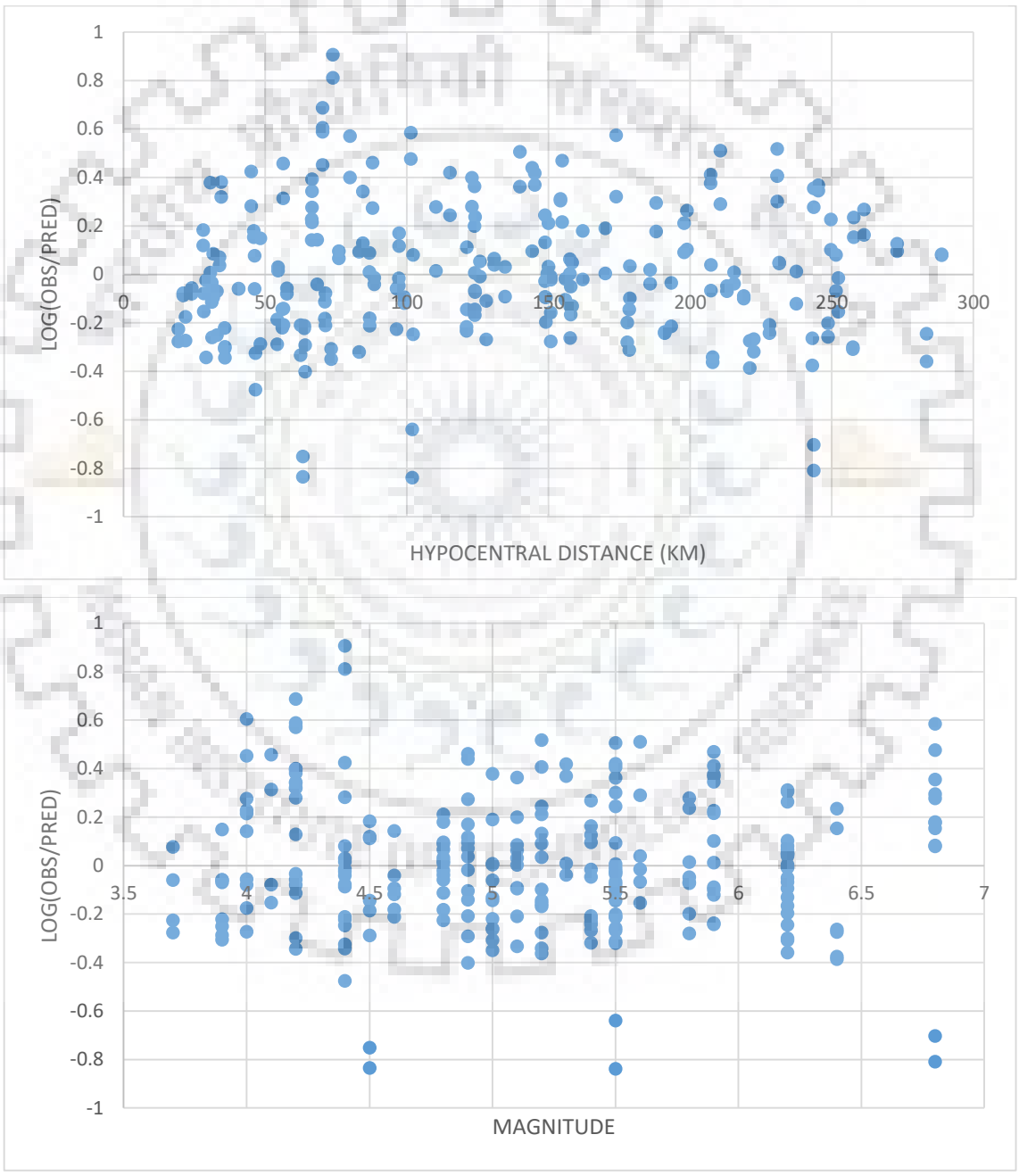

Figure 6.2 Residuals of horizontal PGA between observed values and values predicted by equation (6.1) with hypocentral distance and magnitude.

Above figure shows residual with hypocentral distance and magnitude. The residual here is calculated as:

$$\text{Residual} = \log_{10}\left(\frac{PGA(Observed)}{PGA\ (Predicted)}\right)$$

Where *PGA(Observed)* is the observed recorded value of peak ground acceleration while *PGA(Predicted)* represents the value predicted by empirical attenuation equation. Residual gives the idea of the extent to which the predicted values and the recorded values are consistent. This gives the reliability and applicability of the equation. The plots of residuals against hypocentral distance and magnitude with no apparent trend in residual points shows that the predictive equation is satisfactory.

A simultaneous comparison of the present equation and the equation proposed by M.L. Sharma (1998) for peak horizontal acceleration for Himalayan region in India is shown below. Comparison is done for magnitude 5, 6, 7 and 8. Variation of PGA values with hypocentral distance is shown in graphs. This comparison is done as both the equations are related to a common region and hence can be applied to the same region.

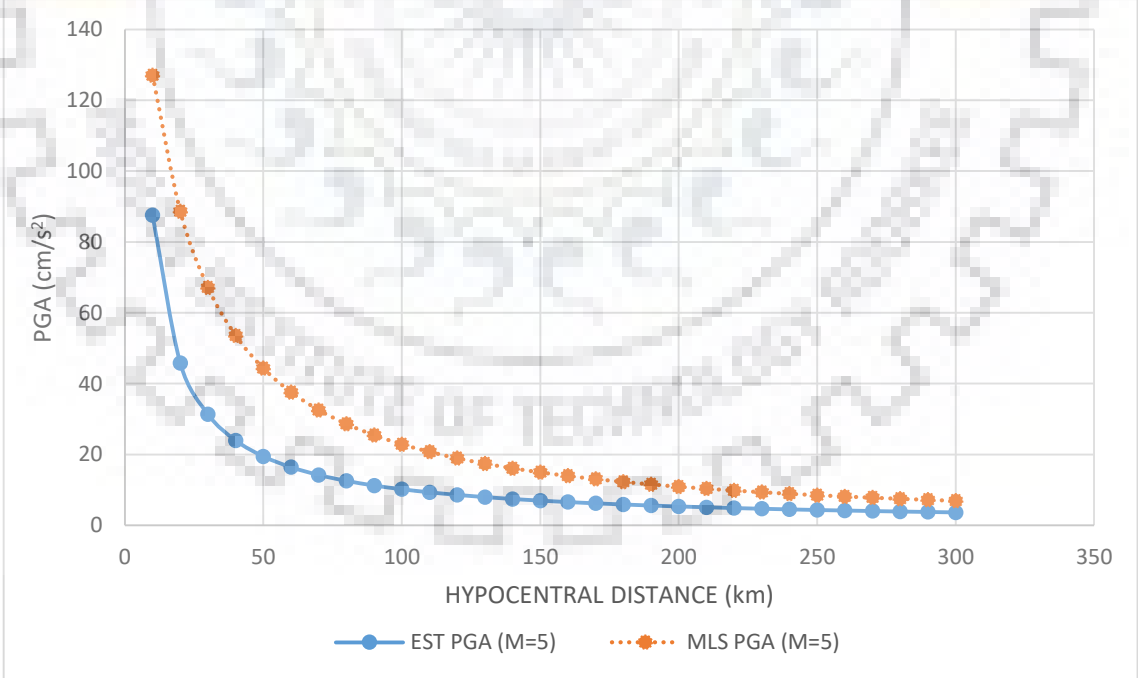

Figure 6.3 Predicted horizontal PGA attenuation curves by equation (6.1) and Sharma (1998) for magnitude M = 5.0 with respect to hypocentral distance.

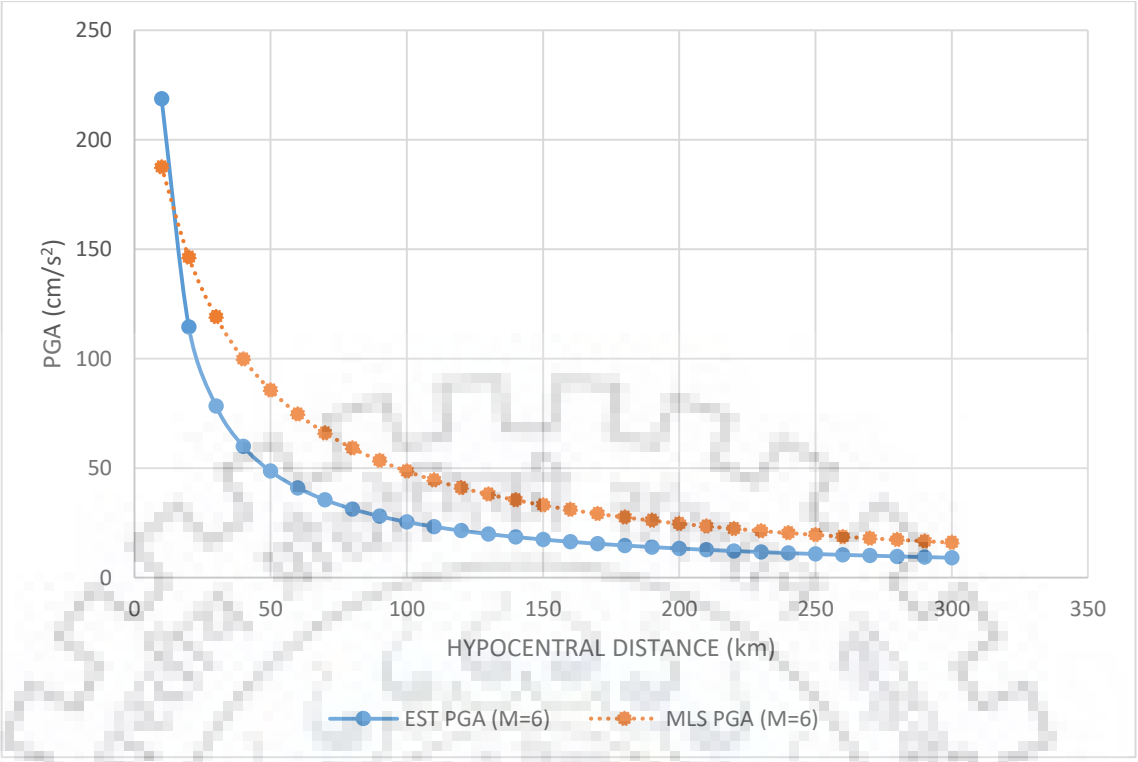

Figure 6.4 Predicted horizontal PGA attenuation curves by equation (6.1) and Sharma (1998) for magnitude M = 6.0 with respect to hypocentral distance.

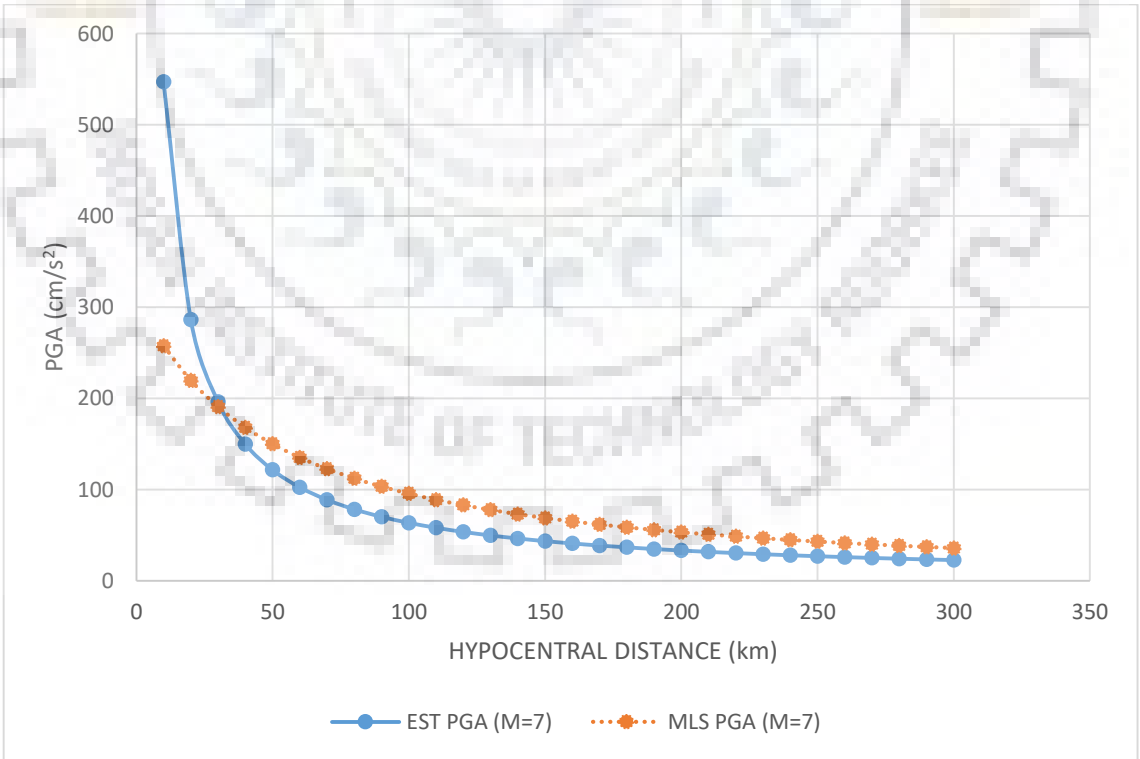

Figure 6.5 Predicted horizontal PGA attenuation curves by equation (6.1) and Sharma (1998) for magnitude M = 7.0 with respect to hypocentral distance.

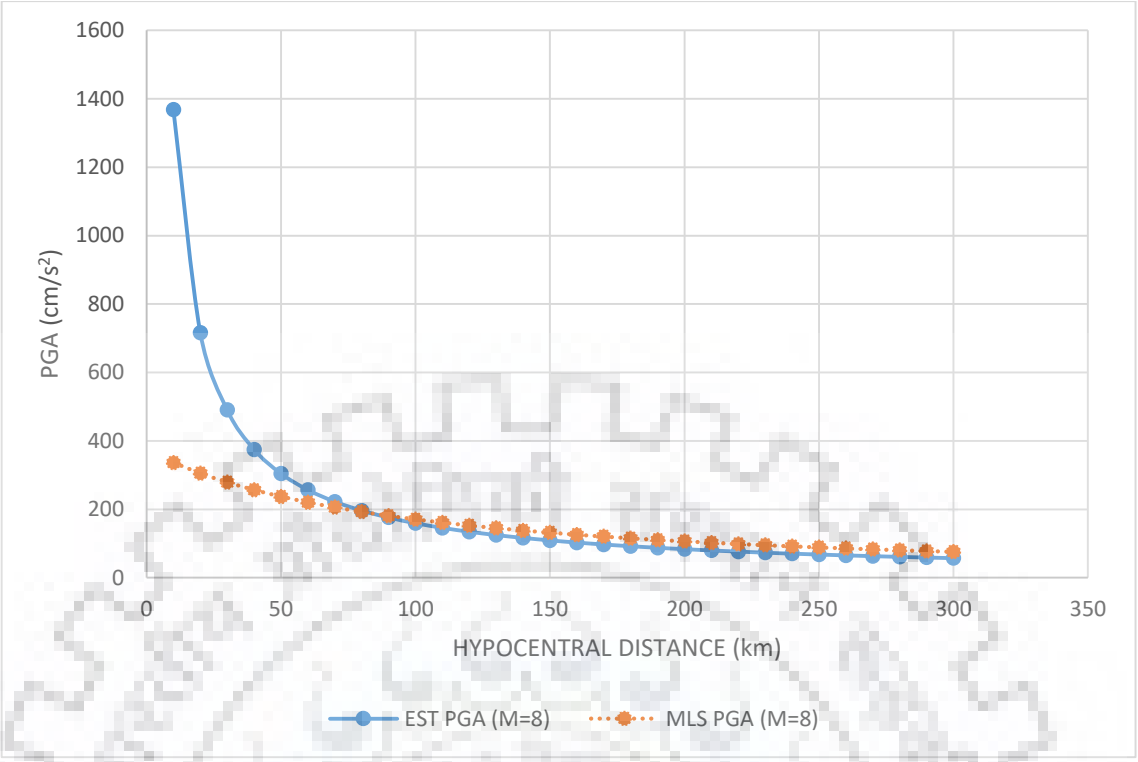

Figure 6.6 Predicted horizontal PGA attenuation curves by equation (6.1) and Sharma (1998) for magnitude M = 8.0 with respect to hypocentral distance.

The above graphs clearly shows that the horizontal PGA predicted by M.L. Sharma (1998) are greater than those predicted by equation (6.1) for magnitudes less than 6. But for magnitudes 6.0 and above predicted values by M. L. Sharma are less than equation (6.1) upto distance 15 km, 30 km and 85 km for magnitudes 6, 7 and 8 respectively. This result is in accordance with the limitation of M. L. Sharma (1998) equation. Predicted horizontal PGA values by M. L. Sharma (1998) are lesser for smaller hypocentral distance. For greater distances both equations predict almost equal horizontal PGA values. Due to larger database, the equation thus obtained in current study is giving more reliable results.

6.2 Taking maximum of the two horizontal components

Considering the maximum of the two horizontal components for the regression analysis will give somewhat larger PGA values. After both steps the final equation obtained can be expressed as:

$$\log_{10}(PGA)=0.9232+0.4154M-0.0021M^{2}-0.9421\log_{10}(R_{HYPO})-0.00113S\pm0.2195 \quad (6.2)$$

where *PGA* is peak ground acceleration in cm/s^2. The standard deviation for the predicted result is 0.2195.

The following graph is showing the attenuation curves of the predicted values with hypocentral distance for magnitudes 5, 6, 7 and 8 for soil site category. As the coefficient of site category is very small equal to 0.00113, it can be ignored. The difference in PGA values for soil and rock site categories are not so distinguishable. The PGA axis is in logarithmic scale and unit is cm/s^2. While the hypocentral axis is in normal scale and unit is in km. The shapes of the curves are independent of the magnitude, showing that the distance decay is independent of magnitude.

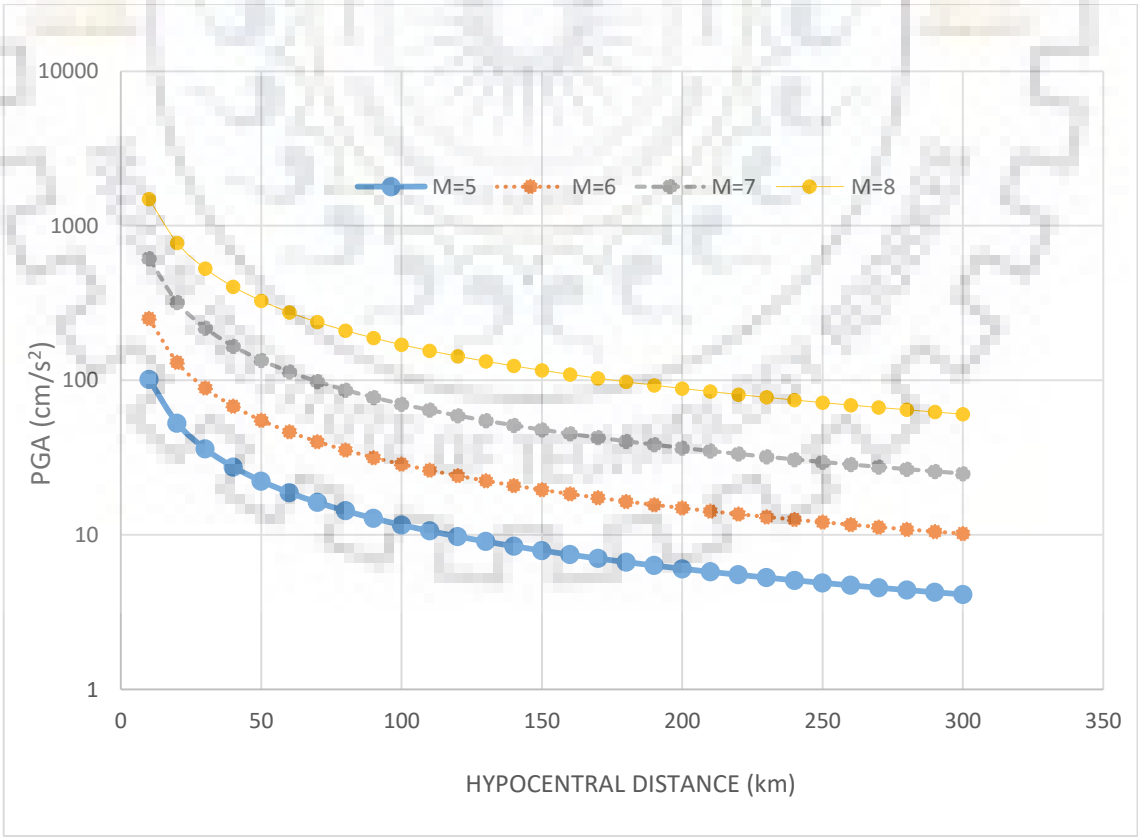

Figure 6.7 Predicted horizontal PGA attenuation curves by equation (6.2) with respect to hypocentral distance for magnitudes (M = 5.0; 6.0; 7.0; 8.0) for soil site.

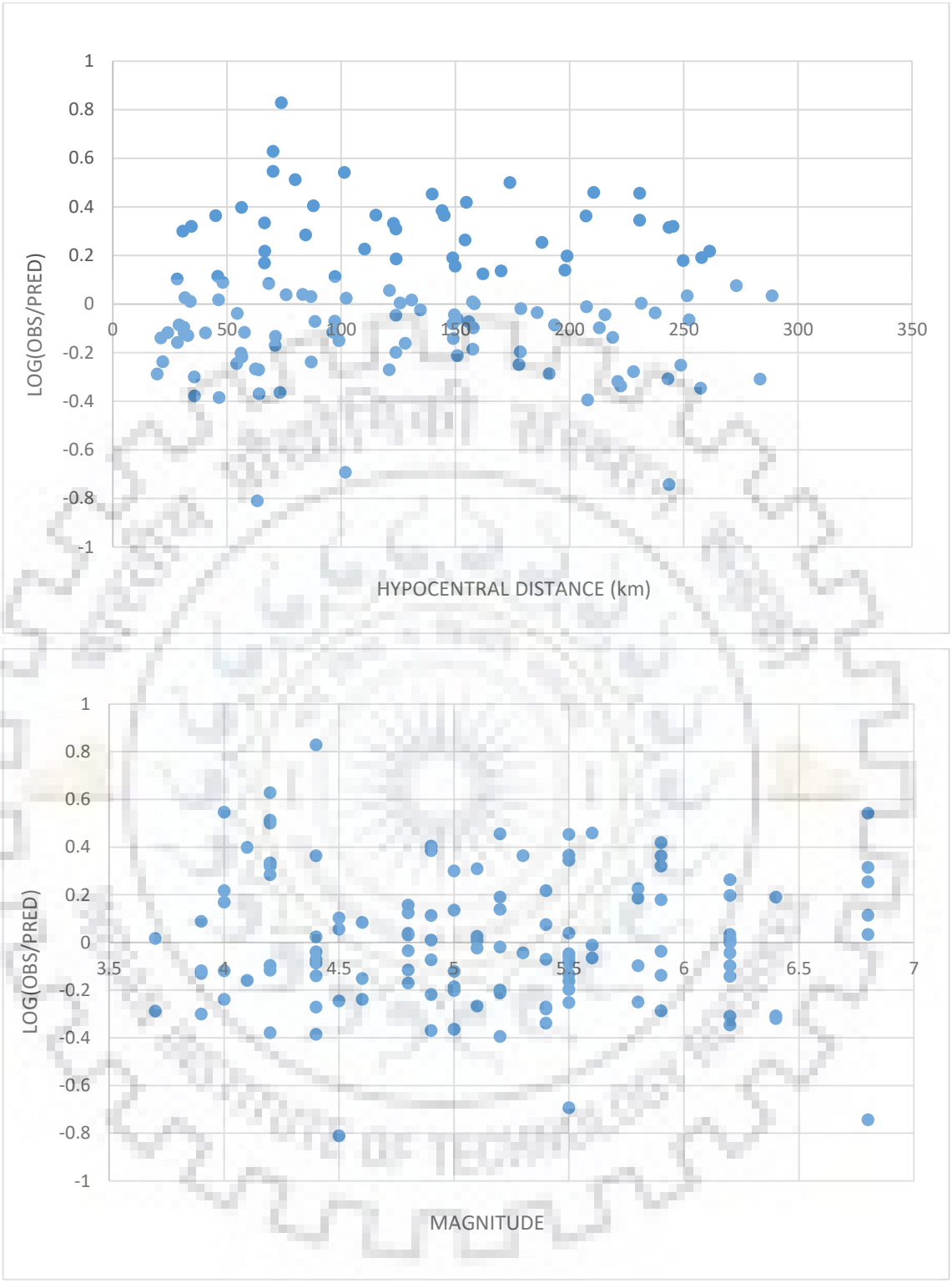

Figure 6.8 Residuals of horizontal PGA between observed values and values predicted by equation (6.2) with hypocentral distance and magnitude.

Here also, the plots of residuals against hypocentral distance and magnitude with no apparent trend in residual points shows that the predictive equation is satisfactory.

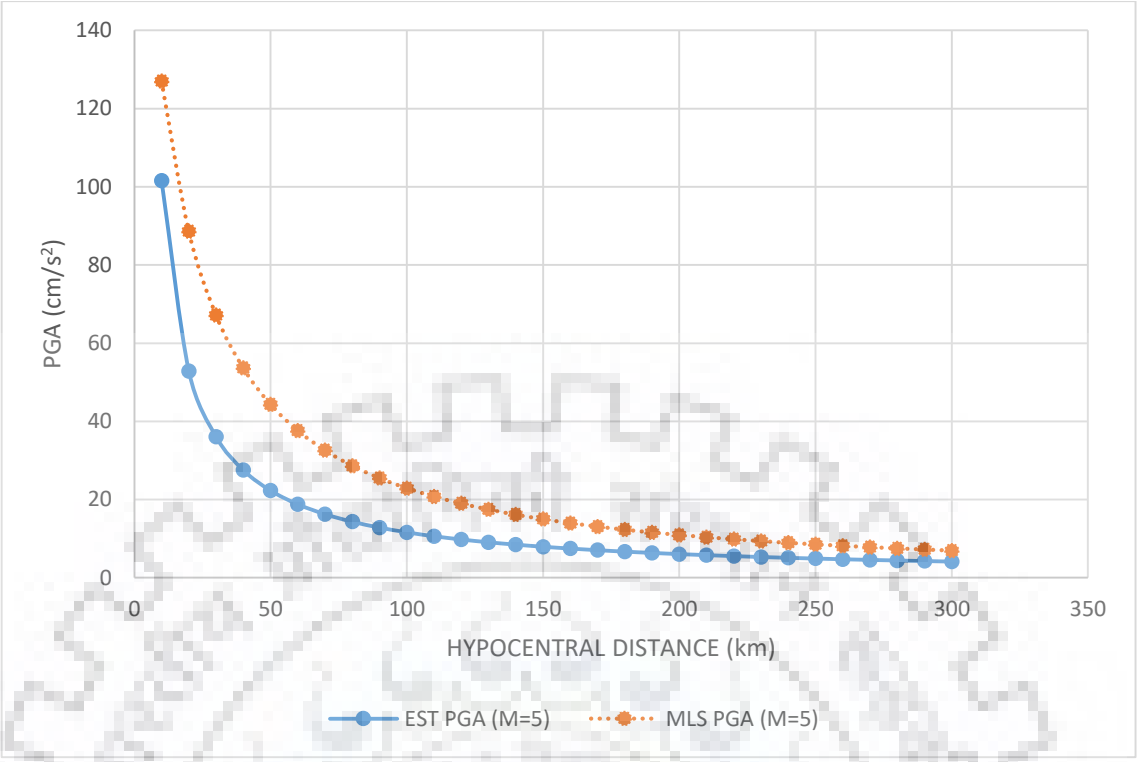

Figure 6.9 Predicted horizontal PGA attenuation curves by equation (6.2) and Sharma (1998) for magnitude M = 5.0 with respect to hypocentral distance.

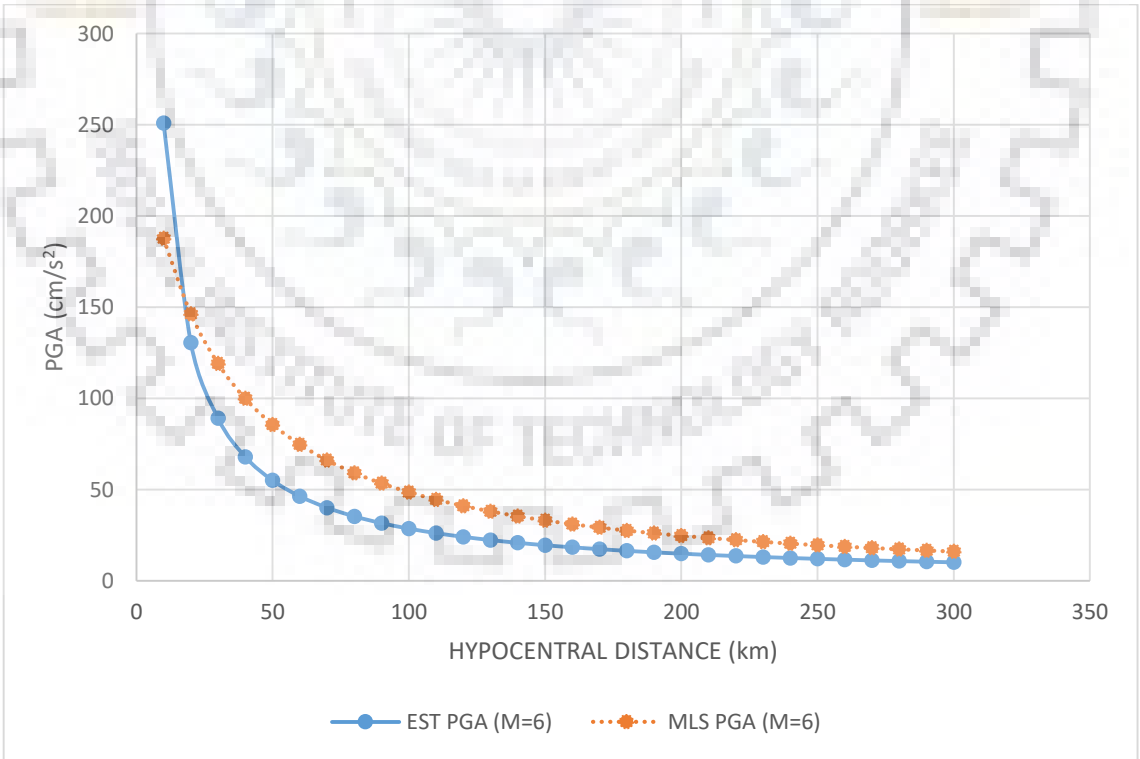

Figure 6.10 Predicted horizontal PGA attenuation curves by equation (6.2) and Sharma (1998) for magnitude M = 6.0 with respect to hypocentral distance.

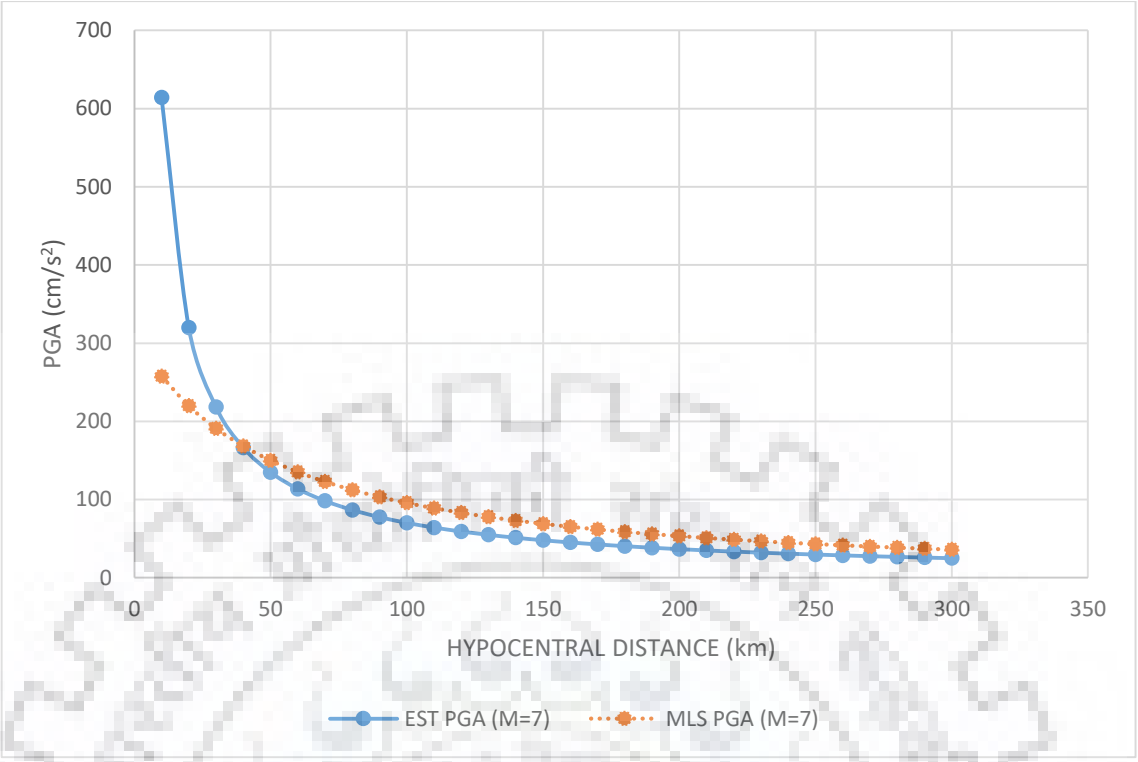

Figure 6.11 Predicted horizontal PGA attenuation curves by equation (6.2) and Sharma (1998) for magnitude M = 7.0 with respect to hypocentral distance.

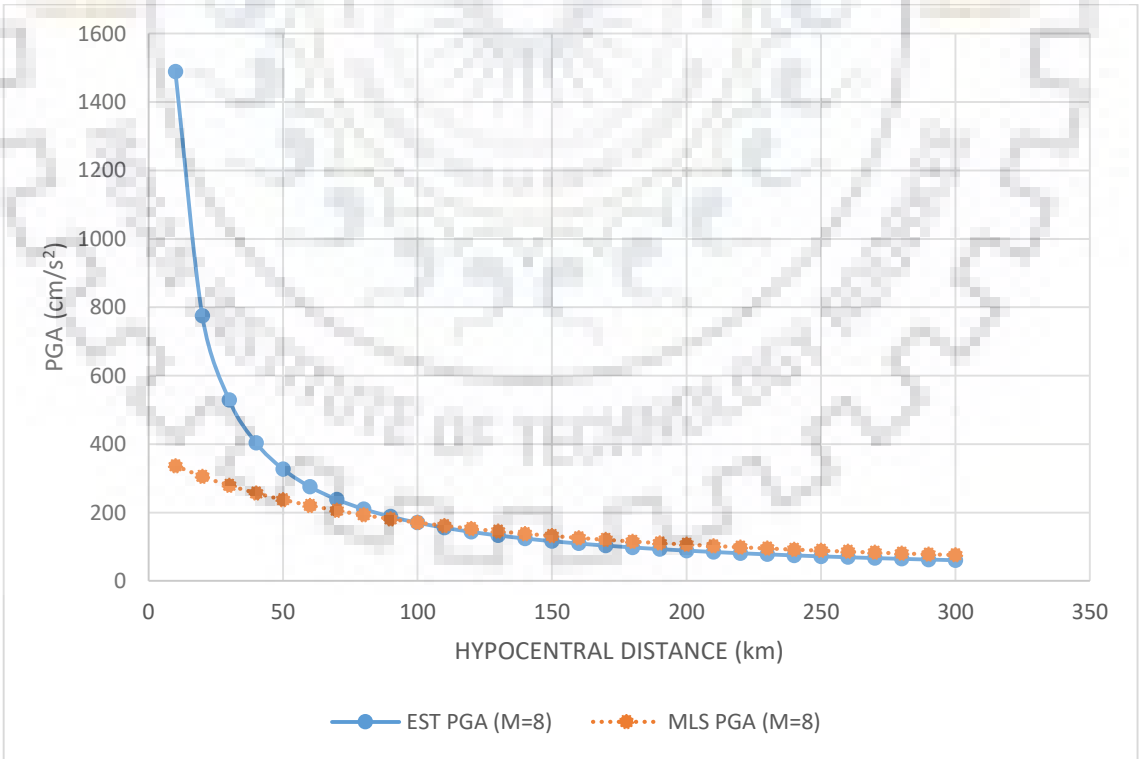

Figure 6.12 Predicted horizontal PGA attenuation curves by equation (6.2) and Sharma (1998) for magnitude M = 8.0 with respect to hypocentral distance.

6.3 Taking mean of the two horizontal components

Here, arithmetic mean of the two horizontal components is taken as the input PGA values. Two-step regression analysis was done and the obtained equation can be expressed as:

$$\log_{10}(PGA) = 0.90082 + 0.3983\,M - 0.93936\log_{10}(R_{HYPO}) - 0.0086\,S \pm 0.210634 \qquad (6.3)$$

where *PGA* is peak ground acceleration in cm/s^2. The standard deviation for the predicted result is 0.210634.

The following graph is showing the attenuation curves of the predicted values with hypocentral distance for magnitudes 5, 6, 7 and 8 for soil site category. As the coefficient of site category is very small equal to 0.0086, it can be ignored. The difference in PGA values for soil and rock site categories are not so distinguishable. The PGA axis is in logarithmic scale and unit is cm/s^2. While the hypocentral axis is in normal scale and unit is in km. The shapes of the curves are independent of the magnitude, showing that the distance decay is independent of magnitude.

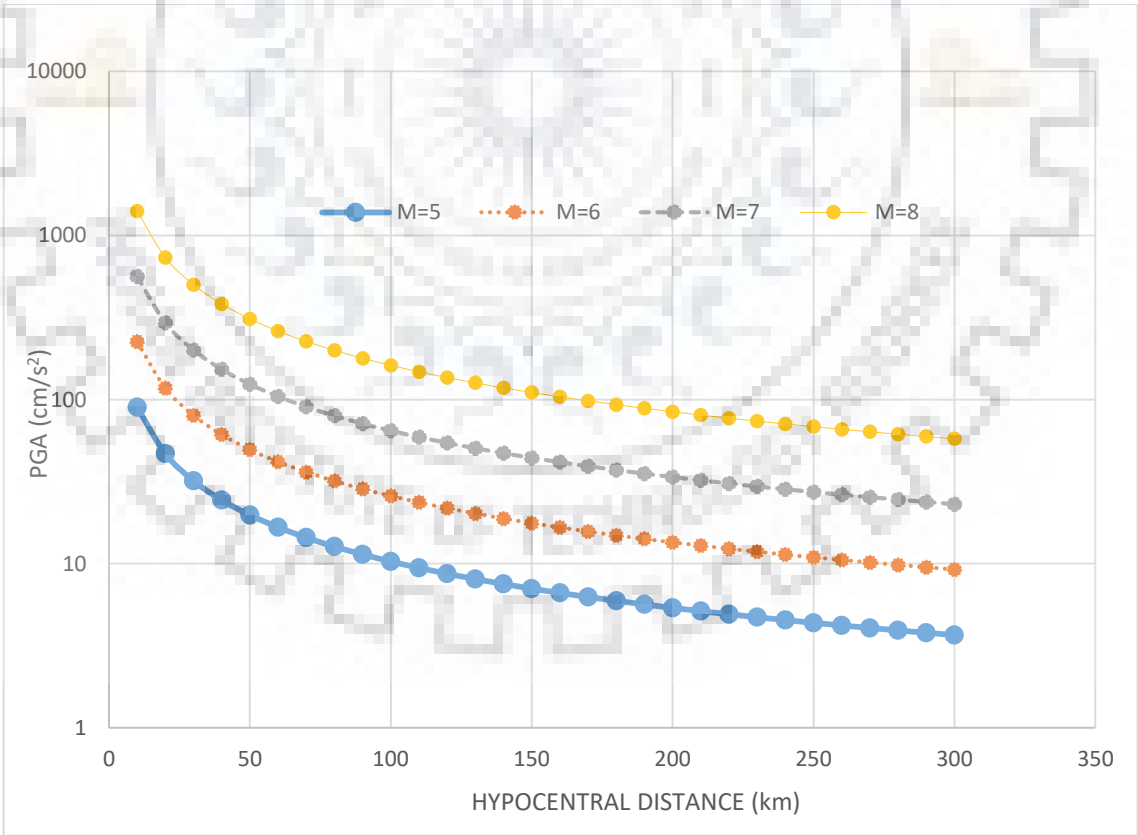

Figure 6.13 Predicted horizontal PGA attenuation curves by equation (6.3) with respect to hypocentral distance for magnitudes (M = 5.0; 6.0; 7.0; 8.0) for soil site.

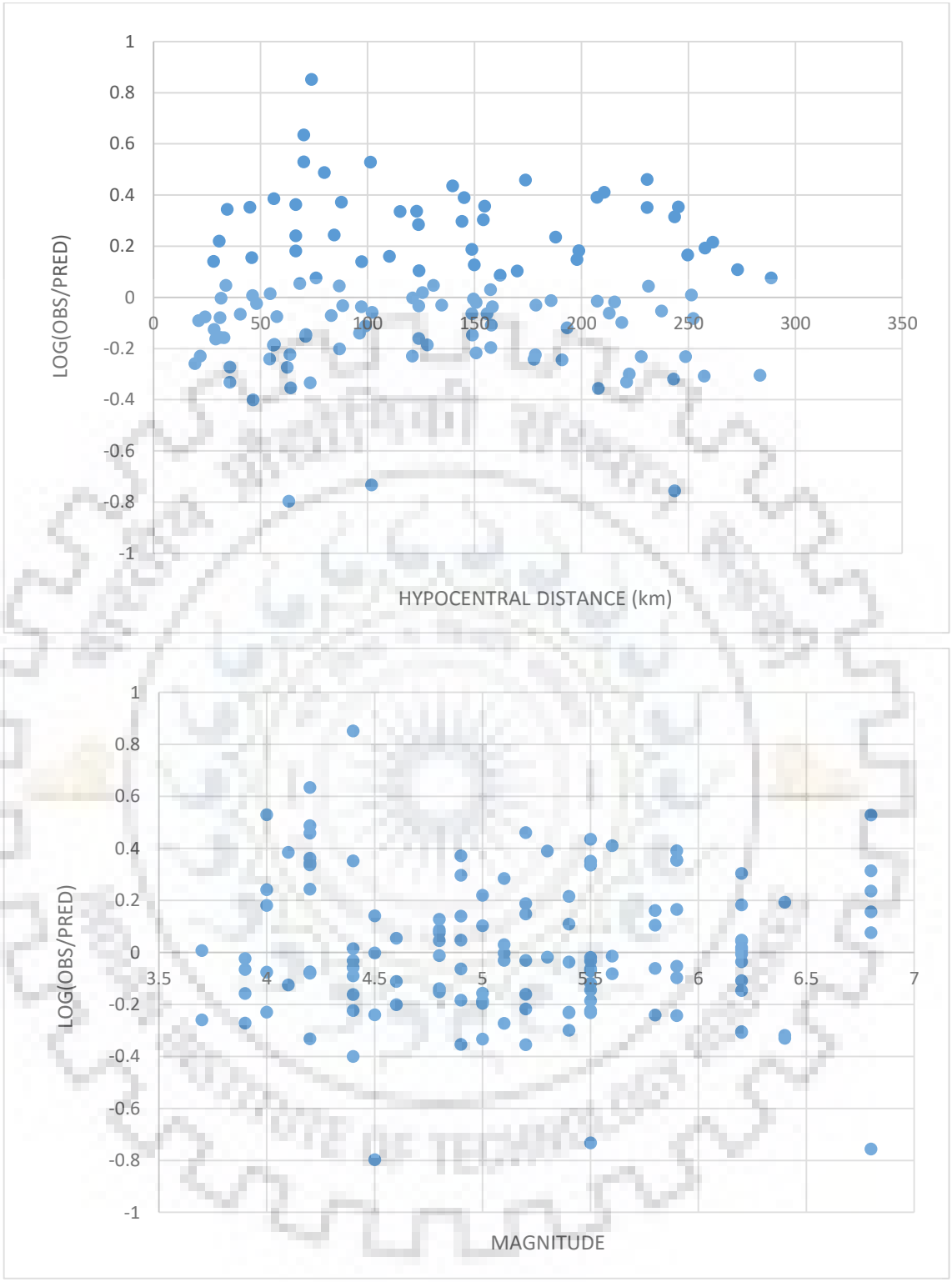

Figure 6.14 Residuals of horizontal PGA between observed values and values predicted by equation (6.3) with hypocentral distance and magnitude.

Here also, the plots of residuals against hypocentral distance and magnitude with no apparent trend in residual points shows that the predictive equation is satisfactory.

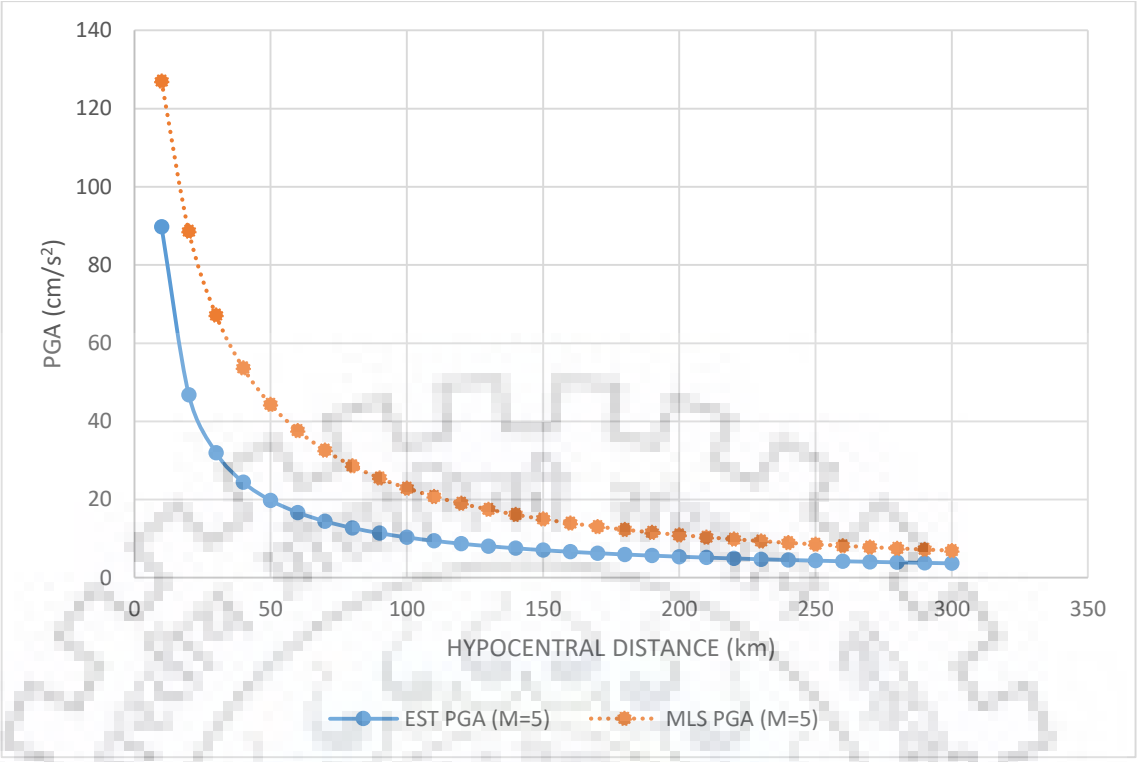

Figure 6.15 Predicted horizontal PGA attenuation curves by equation (6.3) and Sharma (1998) for magnitude M = 5.0 with respect to hypocentral distance.

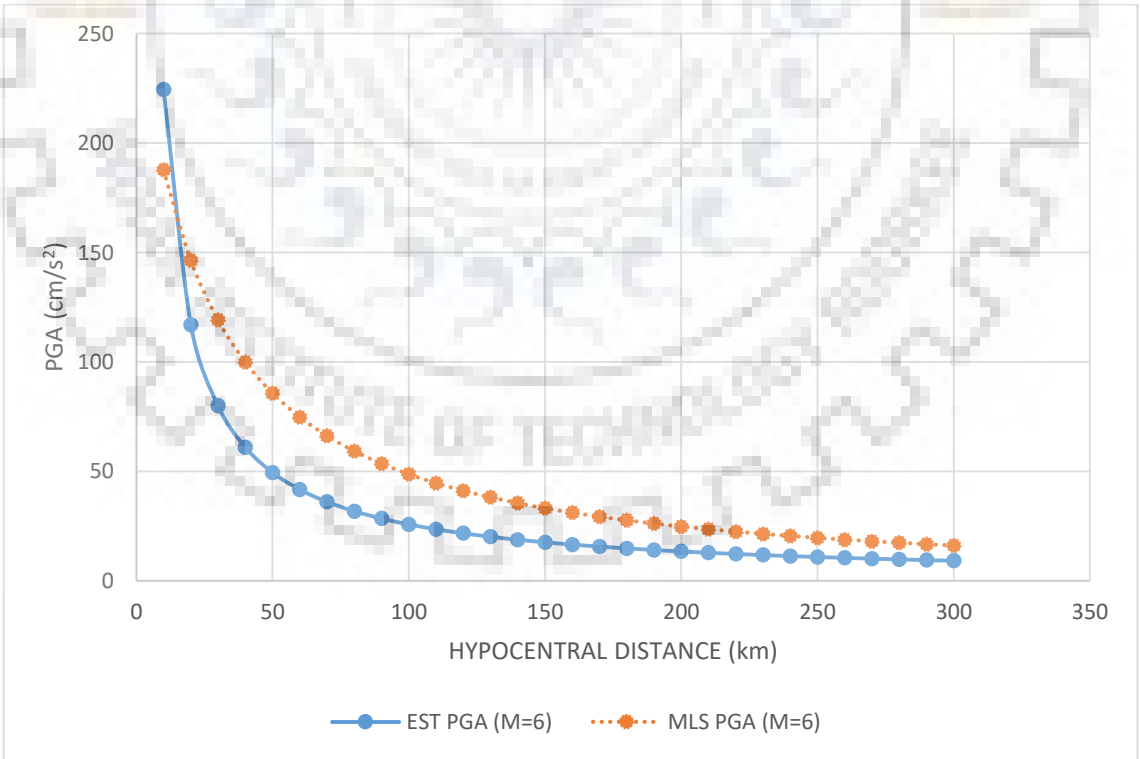

Figure 6.16 Predicted horizontal PGA attenuation curves by equation (6.3) and Sharma (1998) for magnitude M = 6.0 with respect to hypocentral distance.

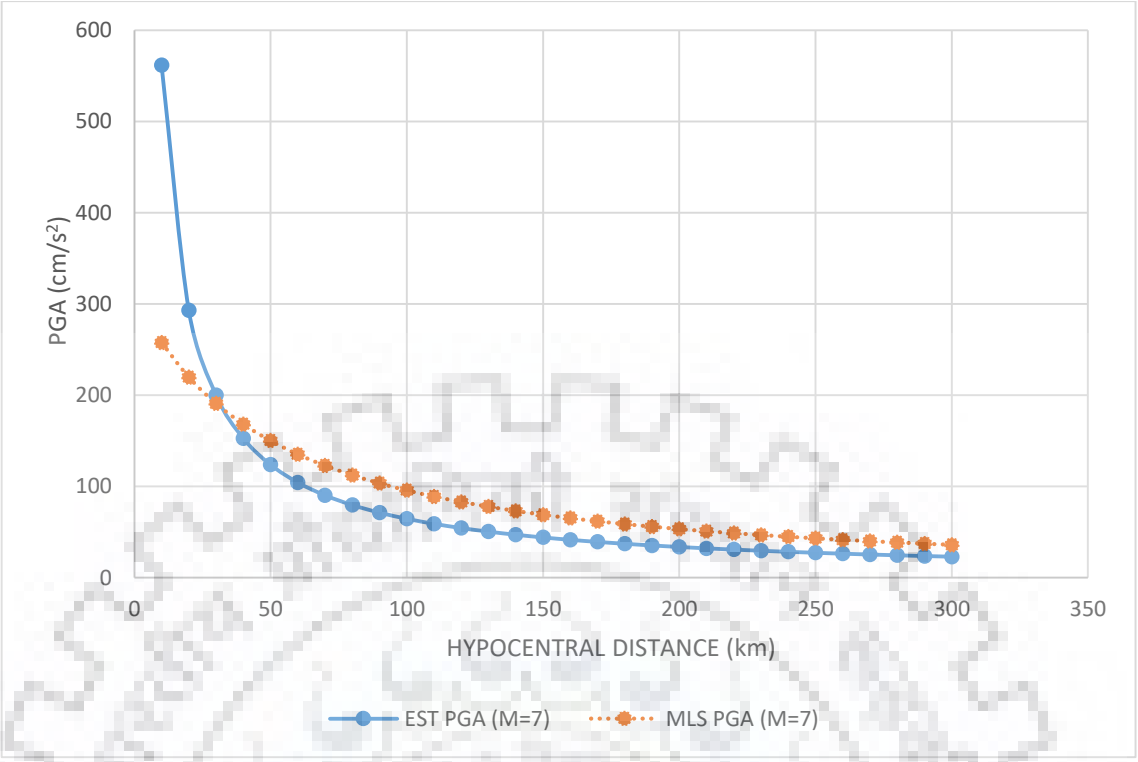

Figure 6.17 Predicted horizontal PGA attenuation curves by equation (6.3) and Sharma (1998) for magnitude M = 7.0 with respect to hypocentral distance.

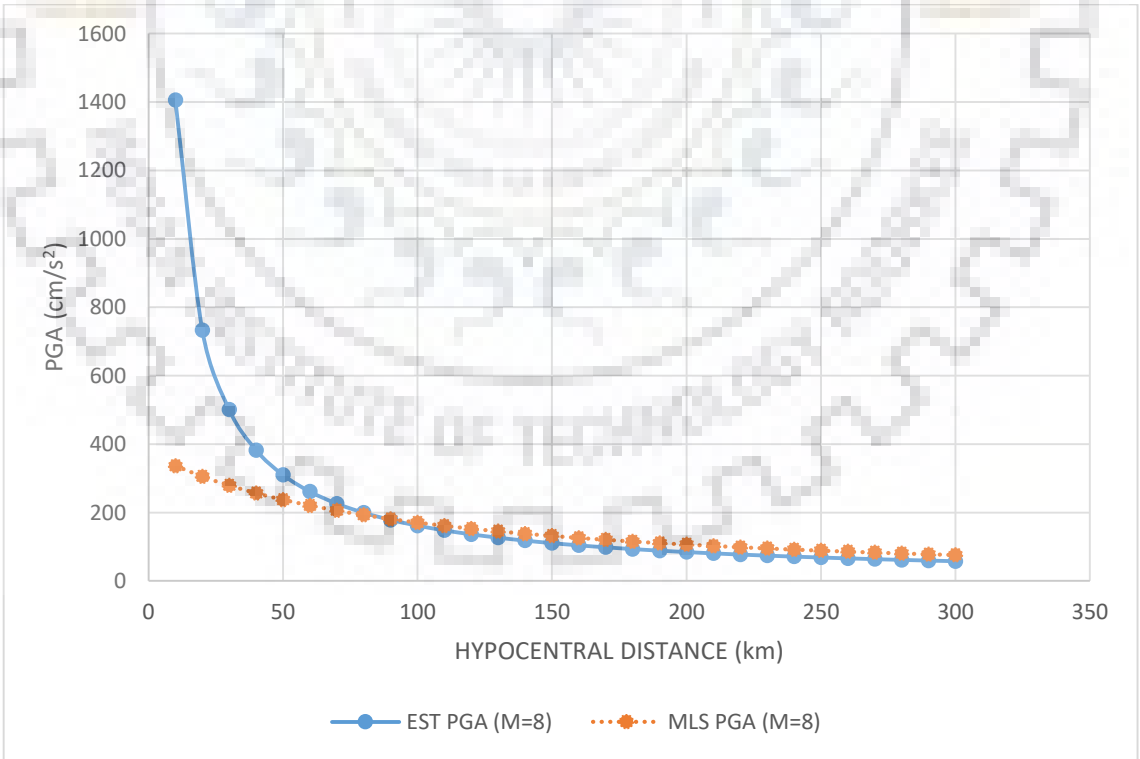

Figure 6.18 Predicted horizontal PGA attenuation curves by equation (6.3) and Sharma (1998) for magnitude M = 8.0 with respect to hypocentral distance.

6.4 Taking SRSS of the two horizontal components

Here, square root of sum of squares of the two horizontal components is taken as the input PGA values. As the input PGA is larger than the two horizontal components individually, we can predict that the equation which will be obtained after the regression will give larger estimates. After the two-step regression analysis, the equation thus obtained can be expressed as:

$$\log_{10}(PGA) = 1.06395 + 0.39844M - 0.94343\log_{10}(R_{HYPO}) - 0.0069S \pm 0.211601 \quad (6.4)$$

where PGA is peak ground acceleration in cm/s^2. The standard deviation for the predicted result is 0.211601.

The following graph is showing the attenuation curves of the predicted values with hypocentral distance for magnitudes 5, 6, 7 and 8 for soil site category. As the coefficient of site category is very small equal to 0.0069, it can be ignored. The difference in PGA values for soil and rock site categories are not so distinguishable. The PGA axis is in logarithmic scale and unit is cm/s^2. While the hypocentral axis is in normal scale and unit is in km. The shapes of the curves are independent of the magnitude, showing that the distance decay is independent of magnitude.

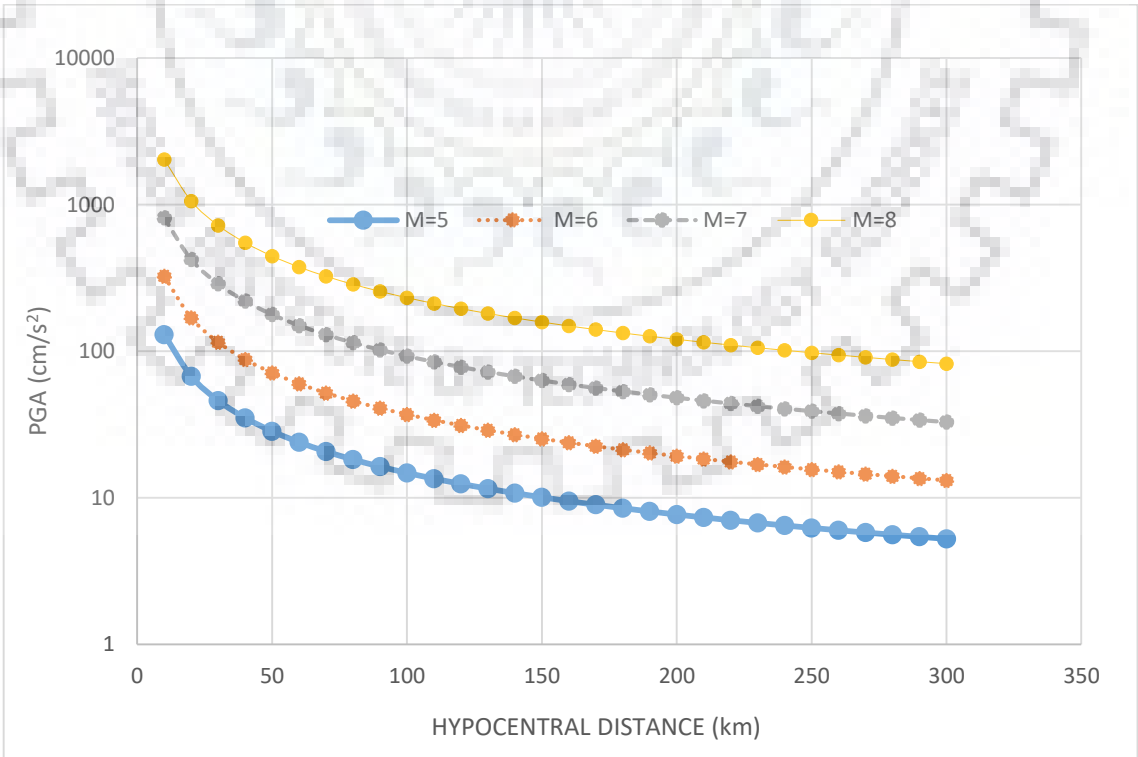

Figure 6.19 Predicted horizontal PGA attenuation curves by equation (6.3) with respect to hypocentral distance for magnitudes (M = 5.0; 6.0; 7.0; 8.0) for soil site.

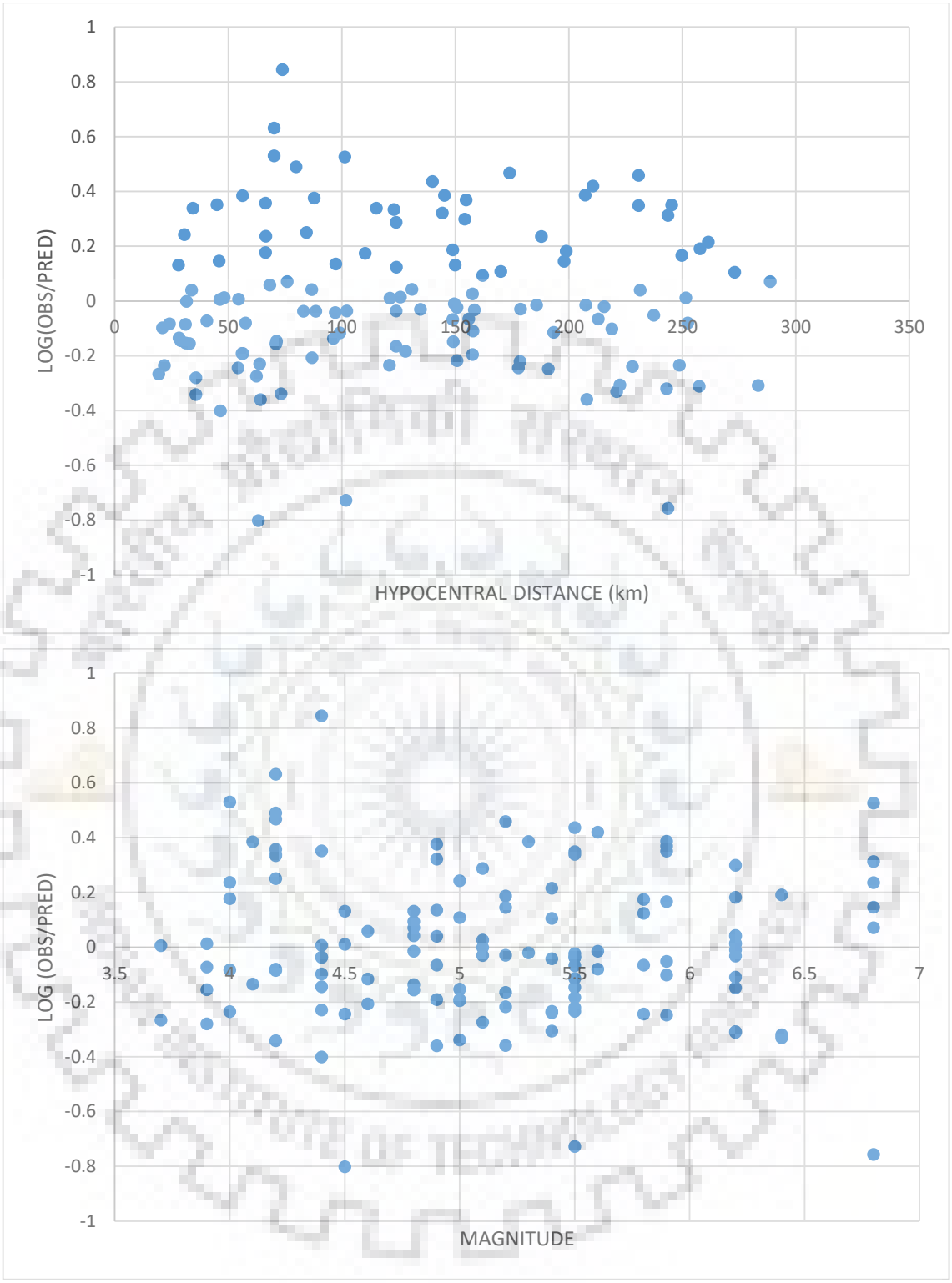

Figure 6.20 Residuals of horizontal PGA between observed values and values predicted by equation (6.4) with hypocentral distance and magnitude.

Here also, the plots of residuals against hypocentral distance and magnitude with no apparent trend in residual points shows that the predictive equation is satisfactory.

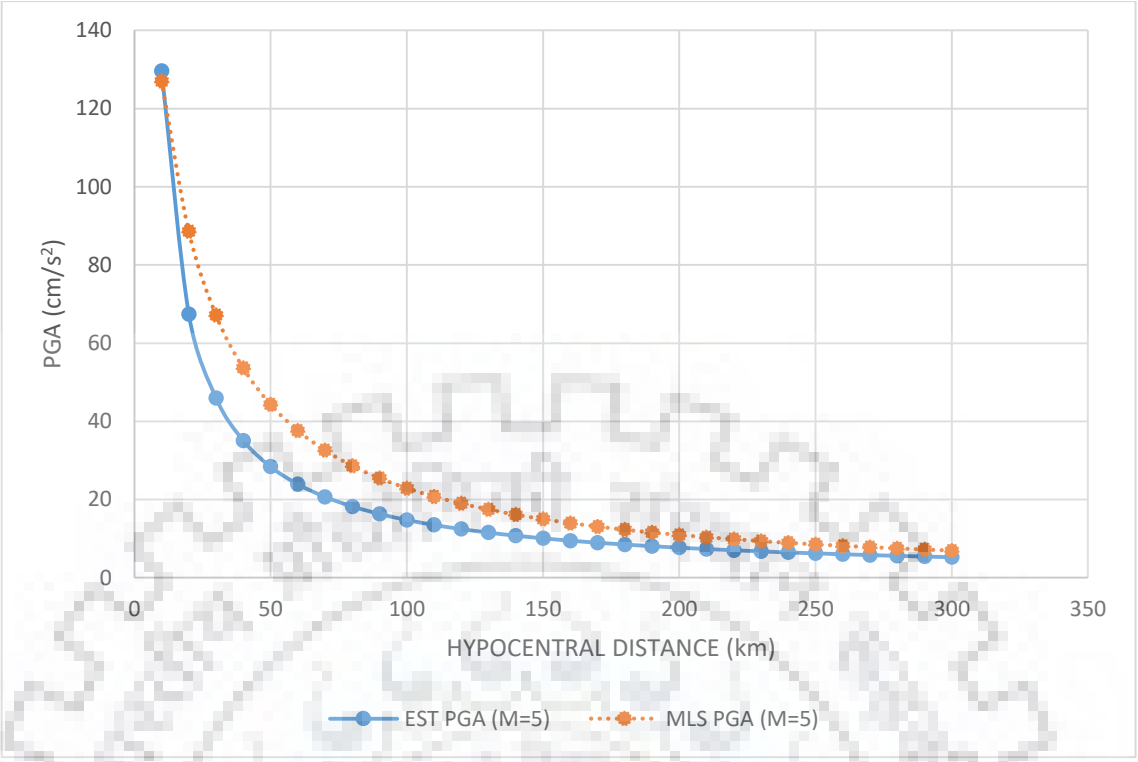

Figure 6.21 Predicted horizontal PGA attenuation curves by equation (6.4) and Sharma (1998) for magnitude M = 5.0 with respect to hypocentral distance.

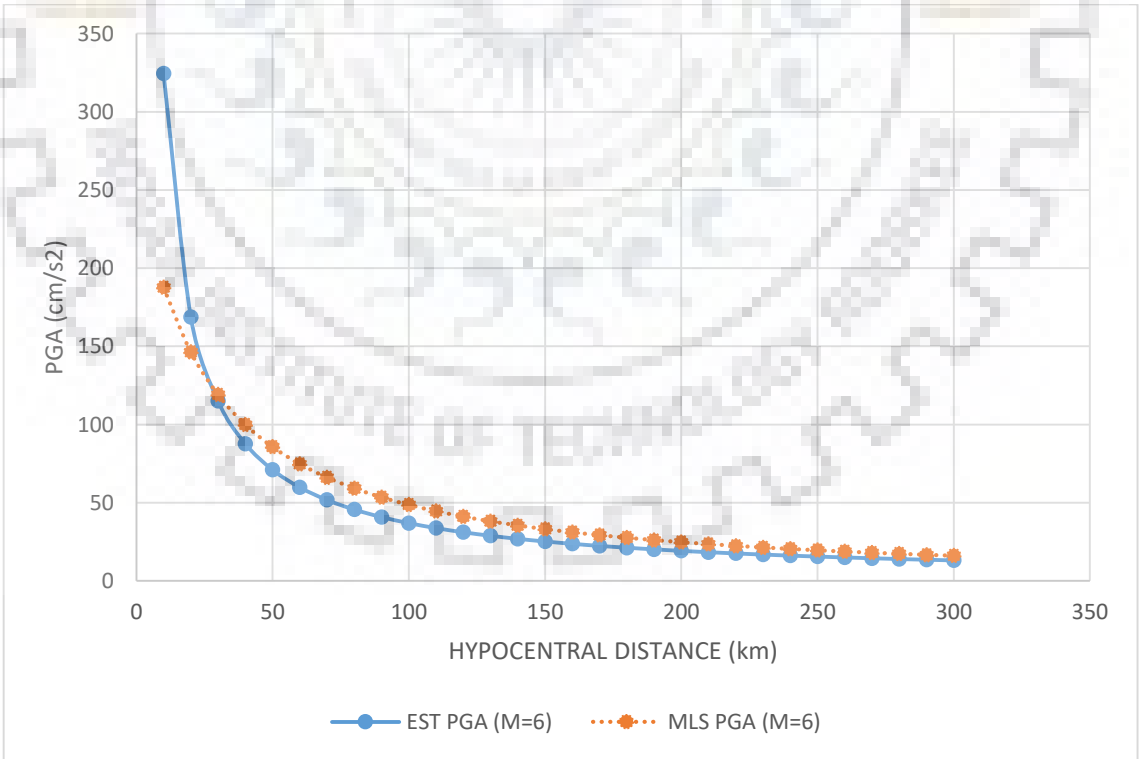

Figure 6.22 Predicted horizontal PGA attenuation curves by equation (6.4) and Sharma (1998) for magnitude M = 6.0 with respect to hypocentral distance.

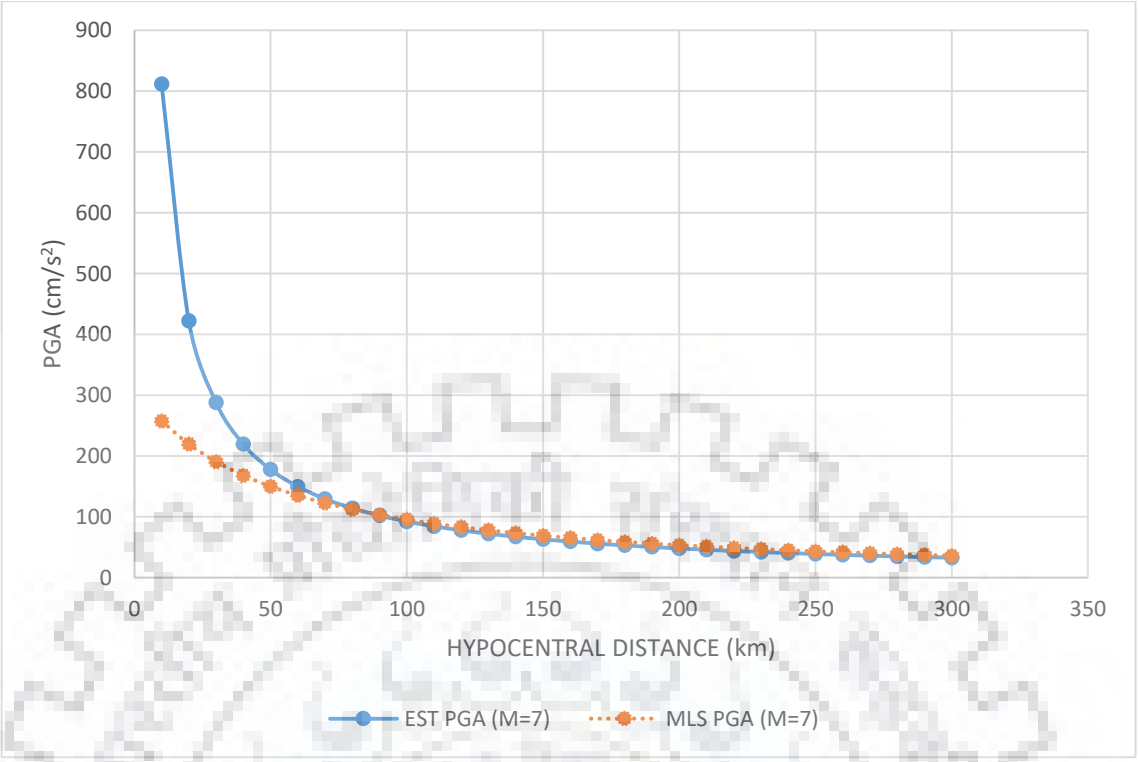

Figure 6.23 Predicted horizontal PGA attenuation curves by equation (6.4) and Sharma (1998) for magnitude M = 7.0 with respect to hypocentral distance.

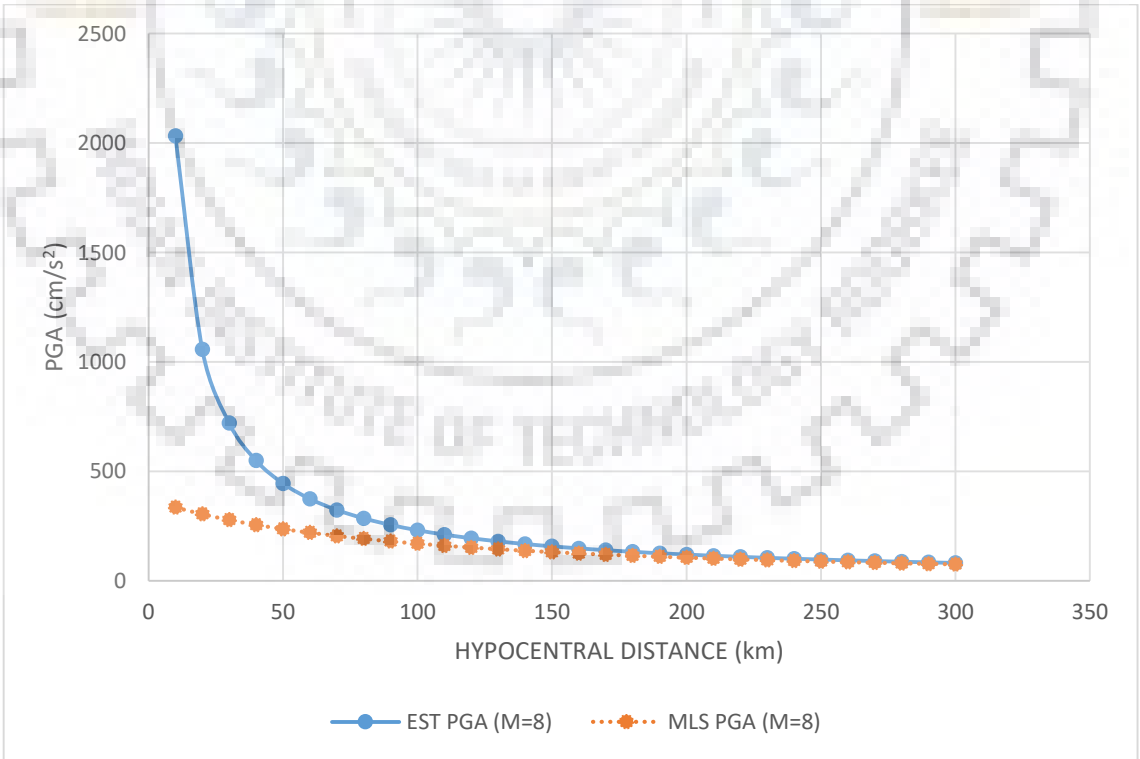

Figure 6.24 Predicted horizontal PGA attenuation curves by equation (6.4) and Sharma (1998) for magnitude M = 8.0 with respect to hypocentral distance.

Chapter 7 CONCLUSION & FUTURE SCOPE

7.1 Conclusion

The conclusive remarks given in Sharma (1998) were that the equation given in that study gives lesser PGA values. At that time, it was suggested that this problem will be minimized in future when a greater data set will be used. A greater dataset is used in the present study i.e. 254 recordings from 52 earthquakes in comparison to 66 recordings from 5 earthquakes in Sharma (1998). We can clearly observe from the plots that the present four equations give quite high values of PGA for almost all magnitudes except below about 5.5. But in SRSS case, the values predicted by equation (6.4) are always higher than those predicted by Sharma (1998).

From the four cases considered and four equations obtained, the equation (6.4) is selected as the final, most reliable and appropriately applicable equation. The reasons for this selection are discussed below:

1. Equation (6.4) gives higher values of horizontal PGA as compared to equation (2.1) for all magnitudes of M = 5 and above.
2. Equation (6.4) has a smaller standard deviation as compared to equations (6.1) and (6.2) but slightly greater than equation (6.3). A smaller standard deviation shows that this equation is more reliable as compared to others.
3. Values predicted by equation (6.4) converges more precisely with values predicted by equation (2.1) for higher distances as compared to equations (6.1), (6.2) and (6.3).
4. As the values predicted by equation (6.4) are higher than those predicted by equations (6.1), (6.2) and (6.3), it is always good to take slightly higher values to be on a safer side when designing structures for earthquakes.
5. Since input PGA was taken as a vectoral combination of the two horizontal components, the predicted value by equation (6.4) can give us the idea about the two horizontal components of the horizontal ground motion.

Thus, the final equation for strong ground motion prediction in North-East Indian region suggested by this study is expressed as:

$$\log_{10}(PGA) = 1.06395 + 0.39844\,M - 0.94343\log_{10}(R_{HYPO}) - 0.0069\,S \pm 0.211601$$

The final conclusions of this study can be summarized as below:

1. This thesis deals with strong ground motion data from North-East Indian region to derive the ground motion attenuation relationship with the predicted parameter as horizontal peak ground acceleration considering four cases which were; (a) taking both components, (b) taking maximum of the two components, (c) taking mean of the two components, and (d) taking square root of sum of squares of the two components. Distance scale was chosen as hypocentral distance. the results are in agreement with the data.
2. The predictive values for soil sites are larger than those of rock sites for given conditions. The amplification effect of soil is thus shown clearly.
3. Plots of the predictive attenuation relationships shows that they are magnitude-independent, i.e. shapes of the curve will not change with magnitude. Also the curves are showing a decaying trend with distance.
4. The predictive equations were compared with some previously suggested equations from the literature. The comparison showed consistency with the previous work.

The main target of this study was to derive the attenuation relationships by the regression analysis of the data selected for North-East Indian region and then compare the results with previously done work and compare the results. The final results show reasonable consistency but there is still some scope of improvement work to be done in future.

7.2 Scope of research in future

Main points to be considered in future studies are discussed below:

1. First of all, as we can observe that coefficient of site category, which is an important factor to be considered in such studies as it describes the effect of local geology on predicted ground motion, is found to be very small in value equals to 0.0069. Reason for this can be the very small number of recording stations located on rock site category (only 4 out of 29 stations). For future studies, it is suggested that more number of recording stations must be located on different types of site categories apart from alluvial soil sites so as to take into account the effects of other sites on ground motion predictions as well.

2. In future, detailed information about earthquake events like, fault type, etc. should be available so that effects of such parameters can also be included in estimating ground motions.
3. More precise instruments should be installed to record the strong motion data so that the standard deviation and spreading of the data can be minimized and the reliability of the equation can be improved.
4. Also there is a need to expand the seismic recording stations network so that other areas can also be studied and new site specific attenuation relationships for those regions can be suggested and used.

This study presented the idea as to how to obtain the attenuation model, covering attenuation mechanism and predictive equation selection methodology. Other methods like least-square one-stage method are also available but two-step regression method was employed due to its aforementioned advantages. Considering more factors will give much more reasonable and reliable results. Also the availability of accurate data is prime prerequisite.

In this research field, source mechanism, wave propagation and site properties are the prime prospects for the improvement of the model. As much study as possible regarding these prospects is done will result in an improved model. Modelling of true aspects of earthquake and ground motion should be considered to modify the attenuation model. Further investigation in this direction is needed. In future, new theories and new technologies may change the research pattern and can lead to new aspects in earthquake engineering. Ground motion attenuation research field needs cooperation at both domestic as well as international level.

In past, we have seen such cooperation being transformed into great breakthroughs in research fields. We just need to assemble and share the knowledge on a common platform so that each research can be directed towards the greater good of mankind.

REFERENCES

1. Abrahamson, N. A., & Silva, W. J. (1997). "Empirical response spectral attenuation relations for shallow crustal earthquakes." *Seismological research letters*, *68*(1), 94-127.
2. Ambraseys, N. N. (1975). "Trends in engineering seismology in Europe." *Pages 39–52 of: Proceedings of Fifth European Conference on Earthquake Engineering*, vol. 3.
3. Atkinson, G. M., & Boore, D. M. (1995). "Ground-motion relations for eastern North America." *Bulletin of the Seismological Society of America*, *85*(1), 17-30.
4. Boatwright, J., & Boore, D. M. (1982). "Analysis of the ground accelerations radiated by the 1980 Livermore Valley earthquakes for directivity and dynamic source characteristics." *Bulletin of the Seismological Society of America*, *72*(6A), 1843-1865.
5. Campbell, K. W. (1982). "Bayesian analysis of extreme earthquake occurrences. Part I and II Probabilistic hazard model." *Bulletin of the Seismological Society of America*, *72*(5), 1689-1705, *73*(4), 1099-1115.
6. Campbell, K. W. (1985). "Strong motion attenuation relations: a ten-year perspective." *Earthquake spectra*, *1*(4), 759-804.
7. Cornell, C. A., Banon, H., & Shakal, A. F. (1979). "Seismic motion and response prediction alternatives." *Earthquake Engineering and Structural Dynamics*, **7**(4), 295–315.
8. Crouse, C. B. (1976). "Horizontal ground motion in Los Angeles during the San Fernando earthquake." *Earthquake Engineering & Structural Dynamics*, *4*(4), 333-347.
9. Douglas, J. (2001). "*A critical reappraisal of some problems in engineering seismology"* (Doctoral dissertation, Imperial College London (University of London)).
10. Esteva, L. (1970). "Seismic risk and seismic design." *Pages 142–182 of:* Hansen, R.J. (ed), *Seismic Design for Nuclear Power Plants*. The M.I.T. Press.
11. Gubbins, D. (1990). "*Seismology and plate tectonics*." Cambridge University Press.
12. Gupta, I. D., & Trifunac, M. D. (2017). "Scaling of Fourier spectra of strong earthquake ground motion in western Himalaya and northeastern India." *Soil Dynamics and Earthquake Engineering*, *102*, 137-159.

13. Joyner, W. B., & Boore, D. M. (1981). "Peak horizontal acceleration and velocity from strong-motion records including records from the 1979 Imperial Valley, California, earthquake." *Bulletin of the Seismological Society of America*, *71*(6), 2011-2038.
14. McGuire, R.K. (1978). "Seismic ground motion parameter relations." *Journal of the Geotechnical Engineering Division, ASCE*, 104 (GT4), 481–490.
15. Petrovski, D., & Marcellini, A. (1988). "Prediction of seismic movement of a site: Statisical approach." *In: Proc. UN Sem. on Predict. of Earthquakes*. Lisbon, Portugal, 14–18 November. Not seen. Reported in Ambraseys & Bommer (1995).
16. Sabetta, F., & Pugliese, A. (1987). "Attenuation of peak horizontal acceleration and velocity from Italian strongmotion records." *Bulletin of the Seismological Society of America*, **77**(5), 1491–1513.
17. Sadigh, K., Chang, C. Y., Egan, J. A., Makdisi, F., & Youngs, R. R. (1997). "Attenuation relationships for shallow crustal earthquakes based on California strong motion data." *Seismological research letters*, *68*(1), 180-189.
18. Sharma, M. L. (1998). "Attenuation relationship for estimation of peak ground horizontal acceleration using data from strong-motion arrays in India." *Bulletin of the Seismological Society of America*, *88*(4), 1063-1069.
19. Sharma, M. L., & Malik, S. (2006). "Probabilistic seismic hazard analysis and estimation of spectral strong ground motion on bed rock in north east India." In *4th international conference on earthquake engineering* (pp. 12-13).
20. Spudich, P., Fletcher, J. B., Hellweg, M., Boatwright, J., Sullivan, C., Joyner, W. B., & Lindh, A. G. (1997). SEA96 – "A new predictive relation for earthquake ground motions in extensional tectonic regimes." *Seismological Research Letters*, *68*(1), 190-198.
21. Trifunac, M. D., & Brady, A. G. (1975). "On correlation of seismoscope response with earthquake magnitude and Modified Mercalli Intensity." *Bulletin of the Seismological Society of America*, *65*(2), 307-321.
22. Ts' ao, H. S. (1980). "Correlations of peak earthquake ground acceleration in the very near field, Agbabian Associates Rept." SAN/1011-125, J El Segundo, California.
23. Verma, R. K., Mukhopadhyay, M., & Ahluwalia, M. S. (1976). "Seismicity, gravity, and tectonics of northeast India and northern Burma." *Bulletin of the Seismological Society of America*, *66*(5), 1683-1694.